Table 2. Correlation between clinical characteristics of TSCC and TGM3 protein expression

Characteristics	Total	Number of TGM3-positive cases (%)	Number of TGM3-negative cases (%)	*P*-values*
Total	53	12 (22.6)	41 (77.4)	
Age (years)				
≤60	27	9 (33.3)	18 (66.7)	0.0994
>60	26	3 (11.5)	23 (88.5)	
Gender				
Male	36	8 (22.2)	28 (77.8)	1.0000
Female	17	4 (23.5)	13 (75.5)	
Stage				
I and II	42	10 (23.8)	32 (76.2)	0.4705
III and IV	11	2 (18.2)	9 (81.8)	
TNM classification				
T category				
T1 and T2	48	12 (25.0)	36 (75.0)	0.5765
T3 and T4	5	0 (0)	5 (100)	
N category				
N0	43	12 (27.9)	31 (72.1)	0.0932
N1-3	10	0 (0)	10 (100)	
Histological grade				
Well	22	9 (40.9)	13 (59.1)	0.0171
Moderate or poor	31	3 (9.7)	28 (90.3)	

**P*-values were calculated by Fisher's exact test and considered statistically significant at <0.05 (two-sided). TGM3, transglutaminase 3; TSCC, tongue squamous cell carcinoma.

with or without 5Aza-dC. However, this had no effect on the restoration of *TGM3* expression, indicating that histone deacetylation is not responsible for the transcriptional silencing of *TGM3* in OSCC cell lines (data not shown).

Methylation status of the CpG island located in the TGM3 gene upstream region. Reversal of gene silencing of *TGM3* by treatment with 5Aza-dC, but not with TSA, indicated that transcription of the *TGM3* gene was regulated through hypermethylation of the *TGM3* gene promoter and/or enhancer in OSCC cells. A database search of the approximately 20-kb sequence of the human *TGM3* gene including the 5′-flanking region identified a CpG-rich region –6433 to –5958 upstream of the transcription start site (Fig. 3c, top, indicated in a green box). This region was a 475-bp-long fragment containing 22 CpG sites (Fig. 3c, middle, indicated by green vertical bars) and had a GC content of 52.5%, thus meeting the proposed criteria for CpG islands.

To examine the DNA methylation status of these CpG sites in OSCC cells, the entire CpG island was sequenced after bisulfite conversion (Fig. 3c, bottom). All of the 22 CpG sites were recurrently methylated in seven cell lines (Ca9-22, HSC-2, HSC-3, HSC-4, HSC-6, KSOC-3, and SAS). The other five cell lines (Ho-1-N-1, Ho-1-u-1, KON, KSOC-2, and SKN-3) showed patchy methylation of CpG sites 1–4 and 9–16. The entire CpG island in normal oral mucosa was largely unmethylated in five out of eight clones examined. Taken together, these findings suggest that silencing of *TGM3* in OSCC cells is likely attributable to the methylation of CpG sites 5–8 and 19–22.

Discussion

In the present study using our 2DICAL proteome platform, we identified CK4, CK13, TGM3, and ANXA1 as proteins whose expression was significantly decreased in microdissected FFPE tissue samples of TSCC. No protein was up-regulated in TSCC on the basis of the current strict criterion ($P < 0.001$, paired *t*-test), indicating the presence of genetic diversity even within such a small number ($n = 10$) of TSCC samples. IHC analysis of an independent cohort revealed that TGM3 expression was markedly decreased in 41 of 53 (77.4%) TSCC cases and that the reduced expression of TGM3 was clearly correlated with loss of histological differentiation. Consistent with these findings, recent studies utilizing a broad range of genomics and proteomics technologies have begun to reveal the importance of down-regulation of TGM3 in SCC including laryngeal carcinoma,[15] head and neck SCC,[16–21] OSCC developing from leukoplakia,[21] and esophageal SCC.[22,23] Reduction or loss of TGM3 expression in SCC has been reportedly correlated with dedifferentiation,[15,22] an increase in the invasive phenotype,[18] a high incidence of lymph-node metastasis,[20,24] and poor prognosis.[23] Together, these findings strongly implicate a crucial role of TGM3 in oral carcinogenesis.

Transglutaminases (TGMs) are a family of Ca^{2+}-dependent enzymes that catalyze protein cross-linking through formation of intermolecular N^{δ}-(γ-glutamyl) lysine isopeptide linkages.[25–27] TGM3 is a zymogen, requiring activation by proteolytic cleavage, and is expressed predominantly in terminally differentiating stratified squamous epithelium.[26–29] TGM3 is essential for cross-linking cornified cell envelope (CCE) protein constituents and formation of the CCE.[30] To date, nine members of the TGM gene family have been identified in the human genome, including TGM1–7, factor XIII, and erythrocyte band 4.2, a catalytically inactive homolog.[26] Despite marked similarities in the genome structures, their distribution, localization, and mechanism for activation of *TGM* genes are highly variable.[26]

We found that transcription of the *TGM3* gene is regulated by DNA methylation. A database search detected only one CpG island located approximately 6 kb upstream of the transcription start site of the *TGM3* gene. Although the promoter of *TGM3* was reported to be located –126 to –91 bp upstream of the transcripton start site,[28] no CpG island was found in the proximal region. Among 22 CpG sites within the CpG island, methylation of CpG sites 5–8 (region 1) and 19–22 (region 2) was correlated with *TGM3* silencing in the OSCC cell lines, reflecting the possibility that one or both of these two regions function as a distal enhancer for *TGM3* transcription. It is intriguing to note that regions 1 and 2 encompass putative elements for transcription factors including GATA-1 and GATA-2, as well as GATA-1, GATA-2,

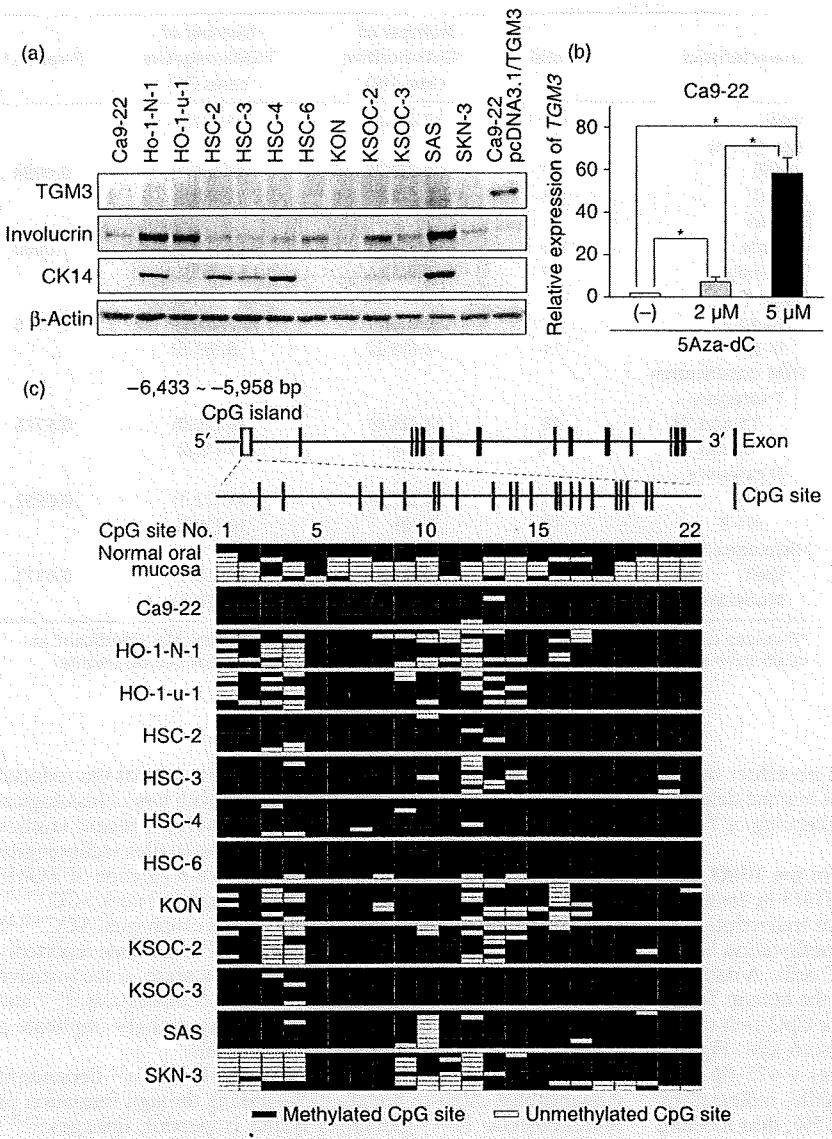

Fig. 3. Epigenetic silencing of transglutaminase 3 (TGM3). (a) TGM3 protein expression in 12 oral squamous cell carcinoma (OSCC) cell lines and Ca9-22 cells transfected with pcDNA3.1/TGM3 (positive control for TGM3). Total cell lysates (10 μg) were analyzed for expression of the indicated proteins by immunoblotting. Involucrin and CK14 were included as epithelial differentiation markers, and β-actin as a loading control. (b) Restoration of TGM3 expression by 5-aza-2′-deoxycytidine (5Aza-dC). Ca9-22 cells were untreated (–) or treated with 2 or 5 μM 5Aza-dC for 5 days. Relative expression levels of the *TMG3* gene were determined by real-time RT-PCR. Columns and bars represent mean ± SD. (c) Cytosine methylation of CpG sites in the upstream region of the *TGM3* gene. Exon/intron structure and the CpG island in the upstream region of the *TGM3* gene are presented schematically (Top). The 22 CpG sites in the CpG island are numbered 1–22 (middle). Genomic DNA was extracted from normal oral mucosa and OSCC cell lines and treated with sodium bisulfite. Eight independent clones per sample were sequenced (bottom). Clear green box, CpG island; vertical blue bars, exons; vertical green bars, CpG sites; clear squares, unmethylated CpG sites; solid squares, methylated CpG sites.

AP-1, and Ets, respectively (www.cbrc.jp/htbin/nph-tfsearch). Transcription factors AP1 and Ets are known to positively regulate epidermal differentiation.[31] It is plausible that tumor-specific hypermethylation in region 2 prevents these transcription factors from binding to their recognition sequences, thereby inactivating transcription of *TGM3*.

Accumulating evidence indicates that TGMs are multifunctional proteins.[26] In fact, some of their functions are even independent of their ability to mediate cross-linking reactions, as exemplified by TGM2, which can function as a molecular switch for transducing cell signaling.[26] TGM2 has been shown to be identical to an atypical high-molecular-weight G-protein known as Ghα, which mediates the activation of phospholipase C through its ability to bind GTP and hydrolyze GTP to GDP.[26,32] Analyses of the crystal structure of TGM3 have indicated that TGM3 possesses a GTP-binding property similar to that of TGM2.[33] TGM3 may also work as a molecular switch governing the cell signaling. *Tgm3* knockout mice show an embryonic-lethal phenotype[34] indicating the non-redundancy of TGM3. This observation also implies that TGM3 has one or more unique functions that cannot be compensated by other TGMs expressed in epithelia, such as TGM1 and TGM5.

Recent advances in proteomic technologies are being increasingly applied to studies of clinical samples in the search for diagnostic biomarkers and therapeutic targets. Here, we have demonstrated for the first time that the powerful combination of the 2DICAL quantitative proteomic high-throughput platform and FFPE archival samples, for which matching clinicopathological information is available, is beginning to show promise.

Acknowledgments

We thank Dr Norihiko Okada (Department of Diagnostic Oral Pathology, Tokyo Medical and Dental University) for advice regarding the design of this study. We also thank Ms Ayako Igarashi, Ms Yuka Nakamura, Ms Satoko Kouda, and Ms Kiyoko Nagumo for their technical assistance. This study was supported by the 'Program for Promotion of Fundamental Studies in Health Sciences' conducted by the National Institute of Biomedical Innovation of Japan, and by the 'Third-Term Comprehensive Control Research for Cancer' and the 'Research on Biological Markers for New Drug Development' conducted by the Ministry of Health, Labor and Welfare of Japan.

Disclosure

None of the authors of this study have a conflict of interest.

doi: 10.1111/j.1349-7006.2009.01227.x

References

1 Forastiere A, Koch W, Trotti A, Sidransky D. Head and neck cancer. *N Engl J Med* 2001; **345**: 1890–900.
2 Spitz MR. Epidemiology and risk factors for head and neck cancer. *Semin Oncol* 1994; **21**: 281–8.
3 Franceschi D, Gupta R, Spiro RH, Shah JP. Improved survival in the treatment of squamous carcinoma of the oral tongue. *Am J Surg* 1993; **166**: 360–5.
4 Mackenzie J, Ah-See K, Thakker N *et al.* Increasing incidence of oral cancer amongst young persons: what is the aetiology? *Oral Oncol* 2000; **36**: 387–9.
5 Annertz K, Anderson H, Biorklund A *et al.* Incidence and survival of squamous cell carcinoma of the tongue in Scandinavia, with special reference to young adults. *Int J Cancer* 2002; **101**: 95–9.
6 Schantz SP, Yu GP. Head and neck cancer incidence trends in young Americans, 1973–97, with a special analysis for tongue cancer. *Arch Otolaryngol Head Neck Surg* 2002; **128**: 268–74.
7 Yamaguchi U, Nakayama R, Honda K *et al.* Distinct gene expression-defined classes of gastrointestinal stromal tumor. *J Clin Oncol* 2008; **26**: 4100–8.
8 Ahram M, Flaig MJ, Gillespie JW *et al.* Evaluation of ethanol-fixed, paraffin-embedded tissues for proteomic applications. *Proteomics* 2003; **3**: 413–21.
9 Patel V, Hood BL, Molinolo AA *et al.* Proteomic analysis of laser-captured paraffin-embedded tissues: a molecular portrait of head and neck cancer progression. *Clin Cancer Res* 2008; **14**: 1002–14.
10 Hwang SI, Thumar J, Lundgren DH *et al.* Direct cancer tissue proteomics: a method to identify candidate cancer biomarkers from formalin-fixed paraffin-embedded archival tissues. *Oncogene* 2007; **26**: 65–76.
11 Ono M, Shitashige M, Honda K *et al.* Label-free quantitative proteomics using large peptide data sets generated by nanoflow liquid chromatography and mass spectrometry. *Mol Cell Proteomics* 2006; **5**: 1338–47.
12 Honda K, Yamada T, Hayashida Y *et al.* Actinin-4 increases cell motility and promotes lymph node metastasis of colorectal cancer. *Gastroenterology* 2005; **128**: 51–62.
13 Shitashige M, Naishiro Y, Idogawa M *et al.* Involvement of splicing factor-1 in β-catenin/T-cell factor-4-mediated gene transactivation and pre-mRNA splicing. *Gastroenterology* 2007; **132**: 1039–54.
14 Huang L, Shitashige M, Satow R *et al.* Functional interaction of DNA topoisomerase IIα with the β-catenin and T-cell factor-4 complex. *Gastroenterology* 2007; **133**: 1569–78.
15 He G, Zhao Z, Fu W, Sun X, Xu Z, Sun K. [Study on the loss of heterozygosity and expression of transglutaminase 3 gene in laryngeal carcinoma]. *Zhonghua Yi Xue Yi Chuan Xue Za Zhi* 2002; **19**: 120–3. (In Chinese.)
16 Gonzalez HE, Gujrati M, Frederick M *et al.* Identification of 9 genes differentially expressed in head and neck squamous cell carcinoma. *Arch Otolaryngol Head Neck Surg* 2003; **129**: 754–9.
17 Choi P, Jordan CD, Mendez E *et al.* Examination of oral cancer biomarkers by tissue microarray analysis. *Arch Otolaryngol Head Neck Surg* 2008; **134**: 539–46.
18 Kondoh N, Ishikawa T, Ohkura S *et al.* Gene expression signatures that classify the mode of invasion of primary oral squamous cell carcinomas. *Mol Carcinog* 2008; **47**: 744–56.
19 Ye H, Yu T, Temam S *et al.* Transcriptomic dissection of tongue squamous cell carcinoma. *BMC Genomics* 2008; **9**: 69.
20 Mendez E, Fan W, Choi P *et al.* Tumor-specific genetic expression profile of metastatic oral squamous cell carcinoma. *Head Neck* 2007; **29**: 803–14.
21 Ohkura S, Kondoh N, Hada A *et al.* Differential expression of the keratin-4-13-14-17 and transglutaminase 3 genes during the development of oral squamous cell carcinoma from leukoplakia. *Oral Oncol* 2005; **41**: 607–13.
22 Liu W, Yu ZC, Cao WF, Ding F, Liu ZH. Functional studies of a novel oncogene TGM3 in human esophageal squamous cell carcinoma. *World J Gastroenterol* 2006; **12**: 3929–32.
23 Uemura N, Nakanishi Y, Kato H *et al.* Transglutaminase 3 as a prognostic biomarker in esophageal cancer revealed by proteomics. *Int J Cancer* 2009; **124**: 2106–15.
24 Uchikado Y, Inoue H, Haraguchi N *et al.* Gene expression profiling of lymph node metastasis by oligomicroarray analysis using laser microdissection in esophageal squamous cell carcinoma. *Int J Oncol* 2006; **29**: 1337–47.
25 Griffin M, Casadio R, Bergamini CM. Transglutaminases: nature's biological glues. *Biochem J* 2002; **368**: 377–96.
26 Lorand L, Graham RM. Transglutaminases: crosslinking enzymes with pleiotropic functions. *Nat Rev Mol Cell Biol* 2003; **4**: 140–56.
27 Esposito C, Caputo I. Mammalian transglutaminases. Identification of substrates as a key to physiological function and physiopathological relevance. *FEBS J* 2005; **272**: 615–31.
28 Lee JH, Jang SI, Yang JM, Markova NG, Steinert PM. The proximal promoter of the human transglutaminase 3 gene. Stratified squamous epithelial-specific expression in cultured cells is mediated by binding of Sp1 and ets transcription factors to a proximal promoter element. *J Biol Chem* 1996; **271**: 4561–8.
29 Hitomi K, Horio Y, Ikura K, Yamanishi K, Maki M. Analysis of epidermal-type transglutaminase (TGase 3) expression in mouse tissues and cell lines. *Int J Biochem Cell Biol* 2001; **33**: 491–8.
30 Kim SY, Chung SI, Steinert PM. Highly active soluble processed forms of the transglutaminase 1 enzyme in epidermal keratinocytes. *J Biol Chem* 1995; **270**: 18026–35.
31 Mack JA, Anand S, Maytin EV. Proliferation and cornification during development of the mammalian epidermis. *Birth Defects Res C Embryo Today* 2005; **75**: 314–29.
32 Nakaoka H, Perez DM, Baek KJ *et al.* Gh: a GTP-binding protein with transglutaminase activity and receptor signaling function. *Science* 1994; **264**: 1593–6.
33 Hitomi K, Ikura K, Maki M. GTP, an inhibitor of transglutaminases, is hydrolyzed by tissue-type transglutaminase (TGase 2) but not by epidermal-type transglutaminase (TGase 3). *Biosci Biotechnol Biochem* 2000; **64**: 657–9.
34 Kim SY, Jeitner TM, Steinert PM. Transglutaminases in disease. *Neurochem Int* 2002; **40**: 85–103.

Supporting Information

Additional Supporting Information may be found in the online version of this article:

Fig. S1. Reproducibility of 2-dimensional image-converted analysis of liquid chromatography and mass spectrometry (2DICAL). The horizontal (x) axis represents the distribution of the peak intensities of a liquid chromatography and mass spectrometry (LC-MS) run (run 1), and the vertical (y) axis represents that of another run (run 2) for the same representative tongue squamous cell carcinoma (TSCC) sample. The average correlation coefficient (CC) of all corresponding 25 018 MS peaks between the duplicates was 0.9992. 94.5% (23 642/25 018) of the peaks are plotted within a two-fold difference (blue lines), and 96.4% (24 117/25 018) within a three-fold difference (red lines).

Fig. S2. Labeled tandem mass spectrometry (MS/MS) spectrum and peak list of ID 4818, which matched the sequences of CK13.

Fig. S3. Labeled tandem mass spectrometry (MS/MS) spectrum and peak list of ID 6588, which matched the sequences of transglutaminase 3 (TGM3).

Fig. S4. Labeled tandem mass spectrometry (MS/MS) spectrum and peak list of ID 13827, which matched the sequences of CK4.

Fig. S5. Labeled tandem mass spectrometry (MS/MS) spectrum and peak list of ID 20149, which matched the sequences of ANXA1.

Fig. S6. Expression of transglutaminase 3 (TGM3) in tongue squamous cell carcinoma (TSCC). The expression of TGM3 protein was evaluated by immunohistochemistry in 53 TSCC cases. Representative images of immunohistochemical staining for TGM3 (a–e) and corresponding HE staining (a′–e′) are aligned side by side (magnification, ×100). TGM3 immunoreactivity was localized predominantly in the cytoplasm and nuclei of non-neoplastic tongue epithelial cells (a). TGM3 is detected in keratinized cancer pearls of some well-differentiated TSCCs (b), but TGM3 immunoreactivity is hardly detectable in moderately (d) or poorly (e) differentiated TSCC.

Please note: Wiley-Blackwell are not responsible for the content or functionality of any supporting materials supplied by the authors. Any queries (other than missing material) should be directed to the corresponding author for the article.

Review Article

Genome-wide DNA methylation profiles in precancerous conditions and cancers

Yae Kanai[1]

Pathology Division, National Cancer Center Research Institute, Tokyo, Japan

(Received August 15, 2009/Revised September 25, 2009/Accepted September 27, 2009/Online publication November 4, 2009)

Alterations of DNA methylation, which result in chromosomal instability and silencing of tumor-related genes, are among the most consistent epigenetic changes observed in human cancers. Analysis of tissue specimens has revealed that DNA methylation alterations participate in multistage carcinogenesis, even from the early and precancerous stages, especially in association with chronic inflammation and/or persistent viral infection, such as chronic hepatitis or liver cirrhosis resulting from infection with hepatitis B or C virus. DNA methylation alterations can account for the histological heterogeneity and clinicopathological diversity of human cancers. Overexpression of DNA methyltransferase 1 is not a secondary result of increased cell proliferative activity, but is significantly correlated with accumulation of DNA hypermethylation in CpG islands of tumor-related genes. Alteration of DNA methyltransferase 3b splicing may result in chromosomal instability through DNA hypomethylation in pericentromeric satellite regions. Genome-wide analysis of DNA methylation status has revealed that the DNA methylation profile at the precancerous stage is basically inherited by the corresponding cancers developing in individual patients. DNA methylation status is not simply altered at the precancerous stage; rather, DNA methylation alterations at the precancerous stage may confer vulnerability to further genetic and epigenetic alterations, generate more malignant cancers, and thus determine patient outcome. Therefore, genome-wide DNA methylation profiling may provide optimal indicators for carcinogenetic risk estimation and prognostication, and thus provide an avenue for cancer prevention and therapy on an individual basis. (*Cancer Sci* 2010; 101: 36–45)

DNA methylation, a covalent chemical modification resulting in addition of a methyl group at the carbon five position of the cytosine ring in CpG dinucleotides, is one of the most consistent epigenetic changes observed in human cancers.[1] DNMTs transfer methyl groups from *S*-adenosylmethionine to cytosines.[2] The preference of DNMT1, a major and well-known DNMT, for hemimethylated over unmethylated substrates *in vitro*,[3] and its targeting of replication foci by binding to PCNA,[4,5] are believed to allow copying of the DNA methylation pattern on the parental strand to the newly synthesized daughter DNA strand. Thus, DNMT1 has been recognized as a "maintenance" DNMT,[6] whereas DNMT3a and DNMT3b show *de novo* DNA methylation activity.[7] DNA methylation normally promotes a highly condensed heterochromatin structure associated with deacetylation of histones H3 and H4, loss of histone H3, lysine 4 (H3K4) methylation, and gain of H3K9 and H3K27 methylation.[8] When methyl-CpG-binding proteins, such as MeCP2[9,10] and MBD2,[11] bind to methylated CpG dinucleotide, their transcriptional repression domain recruits a co-repressor complex containing histone deacetylases. However, histone methyltransferases, such as G9A[12] and SUV39H1,[13] are required to recruit DNMTs. DNA methylation is a stable modification inherited throughout consecutive cell divisions, being essential for the normal development and function of adult organs, particularly for X-chromosome inactivation, genome imprinting, silencing of transposons and other parasitic elements, and proper expression of genes.[14]

Reduction of DNMT1 activity in genetically engineered animals alters the number of tumors or the timing of tumor development, suggesting a causal relationship between DNA methylation alterations and tumorigenesis.[15,16] In 1995, when the *RB* and *VHL* genes were the only tumor suppressor genes known to be silenced by DNA methylation, we showed that the E-cadherin tumor suppressor gene is silenced by DNA methylation around the promoter region.[17] The list of tumor-related genes whose expression levels are altered due to DNA hypo- or hypermethylation is increasing.[18–22] Transcriptionally repressive chromatin modifications within the promoters of tumor-related genes silenced by DNA methylation are known to resemble the chromatin modifications of these genes in normal embryonic stem cells, for example, polycomb complex binding and H3K27 methylation.[23] These genes also have an active marker, H3K4 methylation, in normal stem cells, and this bivalent state is converted to a primary active or repressive chromatin conformation after differentiation cues have been received.[23] During carcinogenesis, such modifications may render the genes vulnerable to errors, resulting in aberrant DNA methylation.[24] DNA hypomethylation induces chromosomal instability through decondensation of heterochromatin and enhancement of chromosomal recombination during carcinogenesis.[25] Translational epigenetics have come of age,[26,27] and empirical analysis of DNA methylation status in clinical tissue samples in connection with the clinicopathological diversity of human cancers is assuming increasing importance for the diagnosis, prevention, and therapy of cancers.[28,29]

Alterations of DNA methylation during multistage carcinogenesis

Alterations of DNA methylation at the precancerous stage. DNA methylation alterations play a key role in the early steps of human carcinogenesis. In the 1990s, although LOH on chromosome 16 was frequently detected by classical Southern blotting in HCCs that were poorly differentiated, large in size, and associated with metastasis,[30] only a few of the molecular events occurring in the earlier stage of hepatocarcinogenesis were known. Since DNA methylation alterations may be correlated with chromosomal instability, we examined the DNA methylation status on chromosome 16 using Southern blotting

[1]To whom correspondence should be addressed.
E-mail: ykanai@ncc.go.jp

doi: 10.1111/j.1349-7006.2009.01383.x

with a DNA methylation-sensitive restriction enzyme. DNA methylation alterations at multiple loci on chromosome 16, compared to normal liver tissue samples, were frequently revealed even in samples of non-cancerous liver tissue showing chronic hepatitis or liver cirrhosis,[31,32] which are widely considered to be precancerous conditions,[33] indicating that DNA methylation alterations are a very early event during multistage hepatocarcinogenesis. This was one of the earliest reports of DNA methylation alterations at the precancerous stage.[31]

DNA hypermethylation around the promoter region of the E-cadherin tumor suppressor gene (16q22.1), which encodes a Ca^{2+}-dependent cell-cell adhesion molecule,[34] has been detected even in samples of non-cancerous liver tissue showing chronic hepatitis or cirrhosis.[35] Heterogeneous E-cadherin expression in such non-cancerous liver tissue, which is associated with small focal areas of hepatocytes showing only slight E-cadherin immunoreactivity, might be due, at least partly, to DNA hypermethylation.[35] Reduction of E-cadherin expression due to DNA methylation around the promoter region may participate even in the very early stage of hepatocarcinogenesis through loss of intercellular adhesiveness and destruction of tissue morphology.

Studies of LOH by PCR using microsatellite markers have been reported, using specimens microdissected from precancerous lesions in several organ types. Whether aberrant DNA methylation precedes chromosomal instability during hepatocarcinogenesis was re-examined using microdissected specimens obtained from lobules, pseudo lobules or regenerative nodules in non-cancerous liver tissue from patients with HCCs by bisulfite modification. Although no degree of DNA methylation of any of the examined C-type CpG islands, which are generally methylated in a cancer-specific but not age-dependent manner, was ever detected in normal liver tissue from patients without HCCs, DNA hypermethylation of such islands was frequently found, even in microdissected specimens of non-cancerous liver tissue showing no remarkable histological changes obtained from patients with HCCs in which LOH was never detected.[36] Thus it was confirmed that aberrant DNA methylation is an earlier event preceding chromosomal instability during hepatocarcinogenesis.

As another example of inflammation-associated carcinogenesis, ductal carcinomas of the pancreas frequently develop after chronic damage due to pancreatitis. At least a proportion of peripheral pancreatic ductal epithelia with an inflammatory background may be at the precancerous stage. When the DNA methylation status of the *p14*, *p15*, *p16*, *p73*, *APC*, *hMLH1*, *MGMT*, *BRCA1*, *GSTP1*, *TIMP-3*, *E-cadherin*, and *DAPK-1* genes was examined, the average number of methylated tumor-related genes and the incidence of DNA methylation of at least one gene were increased in peripheral pancreatic ductal epithelia with an inflammatory background and in another precancerous lesion, PanIN, in comparison with normal peripheral pancreatic duct epithelia.[37]

UCs of the urinary bladder, renal pelvis, and ureter are clinically remarkable because of their multicentricity and tendency to recur (Fig. 1a).[38] A possible mechanism for such multiplicity is the "field effect." Even non-cancerous urothelia showing no remarkable histological changes obtained from patients with UCs can be considered precancerous, because they may have been exposed to carcinogens in the urine. When the DNA methylation status of multiple C-type CpG islands was examined, the average number of methylated C-type CpG islands was increased in non-cancerous urothelia showing no remarkable histological changes obtained from patients with UCs, in comparison with normal urothelia obtained from patients without UCs.[39]

Cigarette smoking is another background factor associated with alterations of DNA methylation during multistage carcinogenesis. DNA hypermethylation at the D17S5 locus, where the *HIC (hypermethylated-in-cancer)-1* tumor suppressor gene was identified, is observed even in non-cancerous lung tissue, which may contain progenitor cells for cancers, obtained from patients with non-small-cell lung cancers. The incidence of DNA hypermethylation in non-cancerous lung tissue obtained from patients with non-small-cell lung cancers is significantly correlated with both smoking history and the extent of pulmonary anthracosis, as an index of the cumulative effects of smoking.[40] Thus, DNA methylation alterations are frequently found even at the precancerous stage in various organs, especially in association with chronic inflammation[41,42] and/or persistent infection with viruses[43–45] or other pathogenic microorganisms, and with cigarette smoking.

DNA methyltransferase 1 overexpression and regional DNA hypermethylation. With respect to the molecular backgrounds of DNA methylation alterations,[46] it has been reported that levels of DNMT1 mRNA expression are significantly higher in samples of non-cancerous liver tissue showing chronic hepatitis or cirrhosis than in normal liver tissue, and are even higher in HCCs.[47,48] The incidence of DNMT1 overexpression in HCCs is significantly correlated with poorer tumor differentiation and portal vein involvement.[49] Moreover, the recurrence-free and overall survival rates of patients with HCCs showing DNMT1 overexpression are significantly lower than those of patients with HCCs that do not.[49]

As mentioned above, at least a proportion of peripheral pancreatic ductal epithelia with an inflammatory background may be at the precancerous stage. The incidence of DNMT1 protein expression increases with progression from peripheral pancreatic ductal epithelia with an inflammatory background, to PanIN, to well-differentiated ductal carcinoma, and finally to poorly differentiated ductal carcinoma of the pancreas, in comparison with normal peripheral pancreatic duct epithelia.[50] DNMT1 overexpression in ductal carcinomas of the pancreas is significantly correlated with the extent of invasion to the surrounding tissue, an advanced stage, and poorer patient outcome.[50] The average number of methylated tumor-related genes in microdissected specimens of peripheral pancreatic ductal epithelia with an inflammatory background, PanIN, and ductal carcinoma was significantly correlated with the level of DNMT1 protein expression examined immunohistochemically in precisely microdissected areas.[37]

Expression levels of DNMT1 mRNA and protein are significantly correlated with poorer differentiation and the CIMP, a cancer phenotype characterized by accumulation of DNA methylation of C-type CpG islands,[51,52] in stomach cancers,[53] but no such association has been observed for the expression of DNMT2, DNMT3a, or DNMT3b.[54] Epstein–Barr virus infection in stomach cancers is significantly associated with marked accumulation of DNA methylation of C-type CpG islands and overexpression of DNMT1 protein.[53] *Helicobacter pylori* infection, another etiologic factor for stomach carcinogenesis, has also been reported to strongly promote regional DNA hypermethylation[55] but is not correlated with DNMT1 expression levels.[53]

It is debatable whether increased DNMT1 expression is due to an increase in the proportion of dividing cells or to an acute increase of DNMT1 expression per individual cancer cell. Immunohistochemical examinations have clearly revealed that the incidence of nuclear DNMT1 immunoreactivity is already higher in non-cancerous urothelia showing no remarkable histological changes obtained from patients with UCs, which may already be exposed to carcinogens in the urine but in which the PCNA labeling index had not yet increased, compared to that in normal urothelia from patients without UCs, indicating that

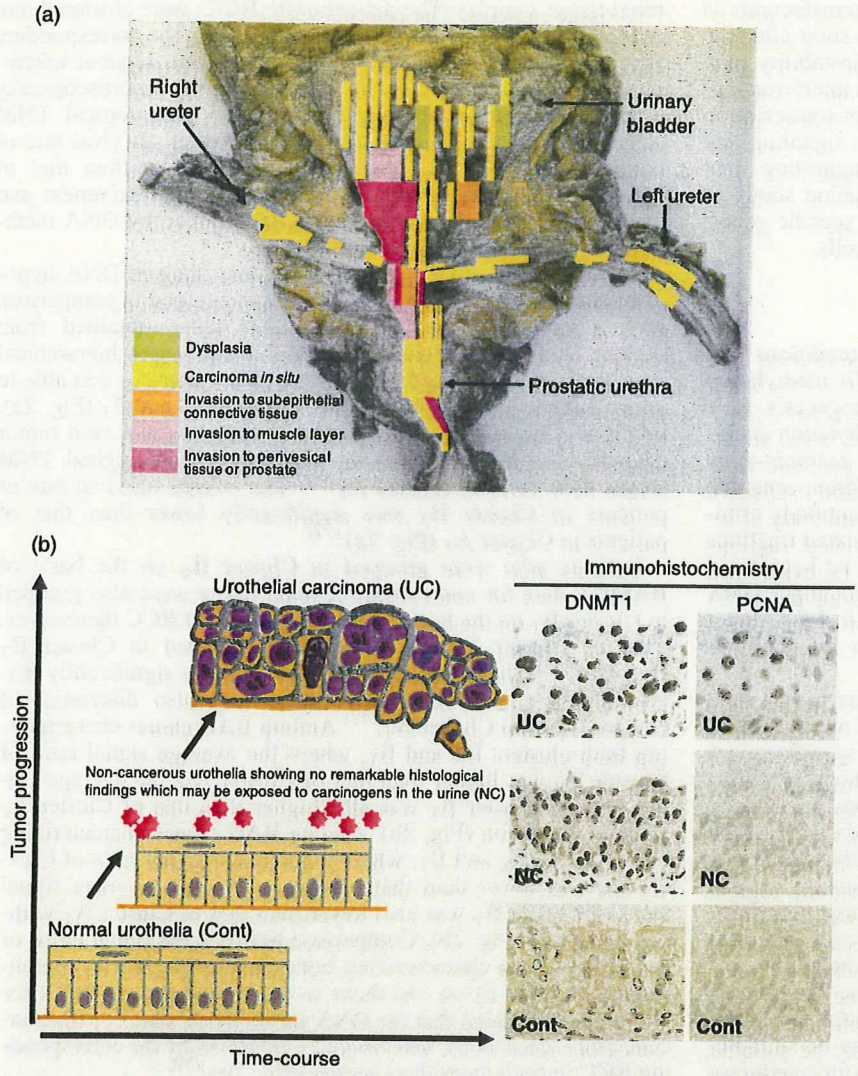

Fig. 1. Overexpression of DNA methyltransferase (DNMT) 1 protein during multistage urothelial carcinogenesis. (a) Specimen obtained by radical cystectomy for multiple urothelial carcinomas (UCs) of the urinary bladder, bilateral ureters, and prostatic urethra. UCs are clinically remarkable because of their multicentricity and tendency to recur: synchronously or metachronously multifocal UCs often develop in individual patients.[38] A possible mechanism for such multiplicity is the "field effect." Even non-cancerous urothelia showing no remarkable histological changes obtained from patients with UCs can be considered precancerous, because they may be exposed to carcinogens in the urine. (b) Immunohistochemical examination for DNMT1 and proliferating cell nuclear antigen (PCNA) in tissue specimens. The incidence of nuclear DNMT1 immunoreactivity had already increased in non-cancerous urothelia showing no remarkable histological changes obtained from patients with UCs (NC), where the PCNA labeling index had not yet increased, compared to that in normal urothelia obtained from patients without UCs (Cont), indicating that DNMT1 overexpression preceded any increase of cell proliferative activity.[56] The intensity of nuclear DNMT1 immunoreactivity was further increased in UCs.[56]

DNMT1 overexpression preceded increased cell proliferative activity (Fig. 1b).[56] The incidence of nuclear DNMT1 immunoreactivity showed a further and progressive increase in dysplastic urothelia, and during transition to UCs (Fig. 1b).[56] Among all examined microdissected specimens of non-cancerous urothelia showing no remarkable histological changes from patients with UCs, or dysplastic urothelia and UCs, accumulation of DNA methylation of C-type CpG islands was significantly correlated with the level of DNMT1 protein expression.[39]

Thus DNMT1 overexpression participates not only in the precancerous stage but also in the malignant progression of various cancers, and has a prognostic impact on patients. DNMT1 overexpression is frequently associated with CIMP of cancers. Although the maintenance activities of DNMT1 are related to its *in vitro* preference for hemimethylated substrates, excessive amounts of DNMT1 in comparison to PCNA may participate in *de novo* methylation of CpG islands. The molecular mechanisms that target DNMT1 to unmethylated substrates in cancers need to be clarified.

Splicing alteration of DNMT3b and DNA hypomethylation in pericentromeric satellite regions. DNA hypomethylation in pericentromeric satellite regions is known to result in centromeric decondensation and enhanced chromosome recombination. In HCCs[57] and UCs,[58] DNA hypomethylation of these regions is correlated with copy number alterations on chromosomes 1 and 9, respectively, where satellite regions are rich. DNMT3b is required for DNA methylation of pericentromeric satellite regions in early mouse embryos, and germline mutations of the *DNMT3b* gene have been reported in patients with immunodeficiency, centromeric instability, and facial anomalies (ICF) syndrome, a rare recessive autosomal disorder characterized by DNA hypomethylation of pericentromeric satellite regions.[59] The major splice variant of DNMT3b in normal liver tissue samples is DNMT3b3, which possesses the conserved catalytic domains.[60] DNMT activity of human DNMT3b3 has been confirmed *in vitro*.[61] In contrast, DNMT3b4 lacks the conserved catalytic domains, although it retains the *N*-terminal domain required for targeting to heterochromatin sites. Samples of normal liver tissue show only a trace level of DNMT3b4 expression.[60] The levels of DNMT3b4 mRNA expression and the ratio of DNMT3b4 mRNA to DNMT3b3 in samples of non-cancerous liver tissue obtained from patients with HCCs, and in HCCs themselves, are significantly correlated with the degree of DNA hypomethylation in pericentromeric satellite regions.[60] DNA demethylation on satellite 2 has been observed in DNMT3b4-transfected human epithelial 293 cells.[60] As DNMT3b4 lacking DNMT activity competes with DNMT3b3 for targeting to pericentromeric satellite regions, DNMT3b4 overexpression may lead to chromosomal instability through induction of DNA hypomethylation in such regions.

doi: 10.1111/j.1349-7006.2009.01383.x

Furthermore, the growth rate of DNMT3b4 transfectants is approximately double that of mock-transfectants soon after the introduction of DNMT3b4, when chromosomal instability may not yet have accumulated.[62] Genes implicated in interferon signaling including signal transducer and activator of transcription (STAT) 1, which acts as an effector of interferon signaling, are upregulated in DNMT3b4 transfectants,[62] suggesting that DNMT3b may act to maintain the DNA methylation status of not only pericentromeric satellite regions but also specific genes, probably in cooperation with DNMT1, in cancer cells.

Genome-wide DNA methylation profiling

DNA methylation profiles in precancerous conditions are inherited by cancers. The above findings that DNA methylation alterations are associated with multistage carcinogenesis have prompted us to carry out genome-wide DNA methylation analysis of tissue specimens. Recently, analysis on a genomic-wide scale has become possible using DNA methylation-sensitive restriction enzyme-based or anti-methyl-cytosine antibody affinity techniques that enrich methylated and unmethylated fractions of genomic DNA.[63,64] These fractions can then be hybridized to DNA microarrays or sequenced. Ultra-high-throughput DNA sequencing technologies are being introduced for the direct sequencing of enriched, methylated fragments or for bisulfite-converted genomic sequencing.[65]

We have used BAMCA.[66–69] Many researchers in this field use the promoter arrays to identify genes that are methylated in cancer cells. However, the promoter regions of specific genes are not the only target of DNA methylation alterations in human cancers. DNA methylation status in genomic regions not directly participating in gene silencing, such as the edges of CpG islands, may be altered at the precancerous stage before the alterations of the promoter regions themselves occur.[70] Genomic regions in which DNA hypomethylation affects chromosomal instability may not be contained in promoter arrays. Moreover, aberrant DNA methylation of large chromosome regions, which are regulated in a coordinated manner in human cancers due to a process of long-range epigenetic silencing, has recently attracted attention.[71] Therefore, we used a BAC array that may be suitable, not for focusing on specific promoter regions, but for overviewing the DNA methylation status of individual large regions among all chromosomes.

When BAMCA methods were applied to samples of non-cancerous renal tissue obtained from patients with clear cell RCCs, many BAC clones showed DNA hypo- or hypermethylation in comparison to normal renal tissue samples from patients without any primary renal tumors.[72] RCCs are usually well demarcated and covered by a fibrous capsule, and hardly ever contain fibrous stroma between cancer cells (Fig. 2a). We were therefore able to obtain cancer cells of high purity from surgical specimens, avoiding contamination with either non-cancerous epithelial cells or stromal cells (Fig. 2a). Therefore, the DNA methylation alterations observed in samples of non-cancerous renal tissue from patients with RCCs cannot be attributable to contamination during sampling. Moreover, DNA methylation alterations in non-cancerous renal tissue did not depend on the distance from the RCC itself to the site from which the non-cancerous renal tissue samples were taken. Because of the lack of any remarkable histological changes or any association with chronic inflammation and persistent infection with viruses or other pathogenic microorganisms, precancerous conditions in the kidney have rarely been described. However, from the viewpoint of DNA methylation, we can consider that non-cancerous renal tissue from patients with RCCs is already at the precancerous stage, showing genome-wide DNA methylation alterations.

We then carried out two-dimensional unsupervised hierarchical clustering analysis based on BAMCA data for non-cancerous renal tissue samples. The patients with RCCs were clustered into two subclasses, clusters A_N and B_N (Fig. 2a). The corresponding RCCs of patients in Cluster B_N showed more frequent macroscopically evident renal vein tumor thrombi, microscopically evident vascular involvement, and higher pathological TNM stages than those in Cluster A_N.[72] The overall survival rate of patients in Cluster B_N was significantly lower than that of patients in Cluster A_N (Fig. 2a).[72] Tumor aggressiveness and even patient outcome might thus be determined by DNA methylation profiles at the precancerous stage.

In RCCs themselves, more BAC clones showed DNA hypo- or hypermethylation, and its degree was increased in comparison with samples of non-cancerous renal tissue obtained from patients with RCCs. Two-dimensional unsupervised hierarchical clustering analysis based on BAMCA data for RCCs was able to group patients into two subclasses, Clusters A_T and B_T (Fig. 2a). RCCs in Cluster B_T more frequently showed renal vein tumor thrombi, vascular involvement, and higher pathological TNM stages than those in Cluster A_T.[72] The overall survival rate of patients in Cluster B_T was significantly lower than that of patients in Cluster A_T (Fig. 2a).[72]

Patients who were grouped in Cluster B_N on the basis of BAMCA data for non-cancerous renal tissue were also grouped in Cluster B_T on the basis of BAMCA data for RCC themselves. That is, Cluster B_N was completely included in Cluster B_T (Fig. 2b).[72] The majority of the BAC clones significantly discriminating Cluster B_N from Cluster A_N also discriminated Cluster B_T from Cluster A_T.[72] Among BAC clones characterizing both clusters B_N and B_T, where the average signal ratio of Cluster B_N was higher than that of Cluster A_N, the average signal ratio of Cluster B_T was also higher than that of Cluster A_T without exception (Fig. 2b). Among BAC clones characterizing both clusters B_N and B_T, where the average signal ratio of Cluster B_N was lower than that of Cluster A_N, the average signal ratio of Cluster B_T was also lower than that of Cluster A_T without exception (Fig. 2b). Comparison between the signal ratios of each BAC clone characterizing both clusters B_N and B_T in non-cancerous renal tissue and those in the corresponding RCCs for all patients revealed that the DNA methylation status of the non-cancerous renal tissue was basically inherited by the corresponding RCC in each individual patient (Fig. 2b).[72]

In non-cancerous renal tissue showing no remarkable histological changes and consisting mainly of renal tubules with specialized functions, no progenitor cell is able to gain a growth advantage, and clonal expansion is unable to occur. Therefore, the distinct DNA methylation profile of Cluster B_N, which is clinicopathologically valid, cannot be established through the selection of one of a number of random DNA methylation profiles in non-cancerous renal tissue in patients with clear cell RCCs, and instead may be established through distinct target mechanisms. As the DNA methylation profiles in Cluster B_T are shared by phenotypically similar patients, who all suffer from clinicopathologically aggressive tumors and show a poor outcome, DNA methylation alterations in at least a proportion of the BAC regions characterizing Cluster B_T cannot be passenger changes. It is clear that cancer itself can induce alterations in DNA methylation. However, DNA methylation alterations of BAC regions characterizing Cluster B_T may significantly participate in carcinogenesis, as the DNA methylation profile in Cluster B_N was established at a very early and precancerous stage of carcinogenesis and inherited during progression of the cancers themselves as Cluster B_T. At least a proportion of DNA methylation alterations at the precancerous stage may be "epigenetic gatekeepers"[21] and which allow time for further epigenetic and genetic alterations including genetic gatekeeper mutations (Fig. 3).

In fact, when the DNA methylation status of C-type CpG islands was examined,[73] the average number of methylated

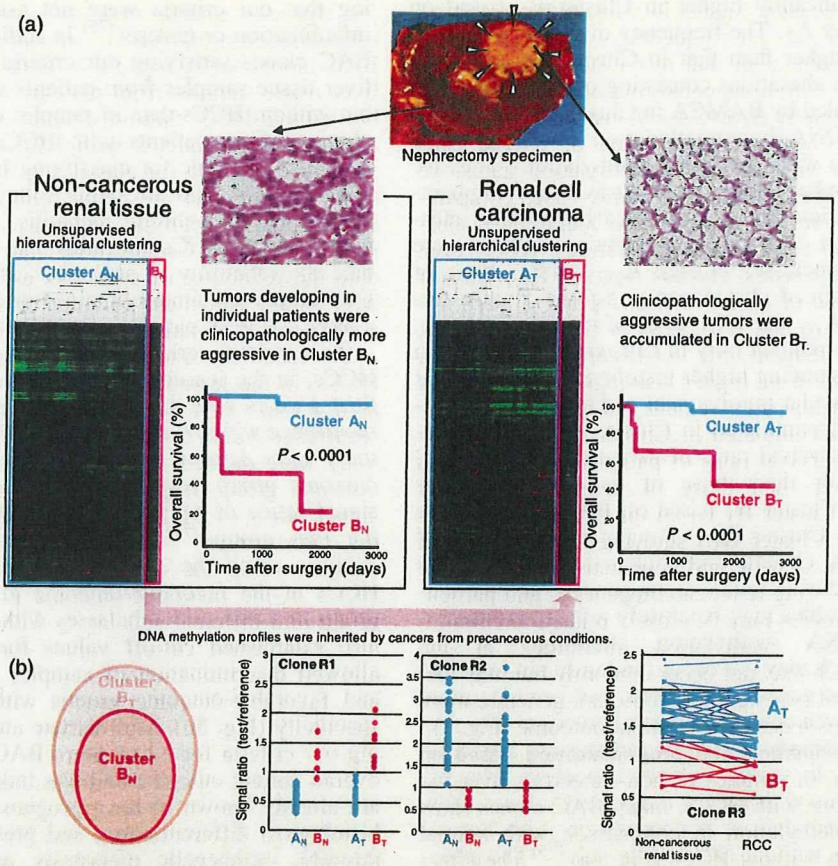

Fig. 2. DNA methylation profiles in precancerous conditions and renal cell carcinomas (RCCs). (a) Bacterial artificial chromosome array-based methylated CpG island amplification (BAMCA) data for tissue samples obtained from patients with RCCs (arrowheads). Using unsupervised hierarchical clustering analysis based on BAMCA data for samples of their non-cancerous renal tissue, patients with RCCs were clustered into two subclasses, Clusters A_N and B_N.[72] Clinicopathologically aggressive RCCs were accumulated in Cluster B_N, and the overall survival rate of patients in Cluster B_N was significantly lower than that of patients in Cluster A_N.[72] Using unsupervised hierarchical clustering analysis based on BAMCA data for their RCCs, patients were clustered into two subclasses, Clusters A_T and B_T.[72] Clinicopathologically aggressive clear cell RCCs were accumulated in Cluster B_T, and the overall survival rate of patients in Cluster B_T was significantly lower than that of patients in Cluster A_T.[72] (b) Correlation between DNA methylation profiles of precancerous conditions and those of RCCs. Cluster B_N was completely included in Cluster B_T (left panel). The majority of the bacterial artificial chromosome (BAC) clones, 724 in all, significantly discriminating Cluster B_N from Cluster A_N, also discriminated Cluster B_T from Cluster A_T.[72] In 311 of the 724 BAC clones, where the average signal ratio of Cluster B_N was higher than that of Cluster A_N, such as Clone R1 in the middle panel, the average signal ratio of Cluster B_T was also higher than that of Cluster A_T without exception.[72] In 413 of the 724 BAC clones, where the average signal ratio of Cluster B_N was lower than that of Cluster A_N, such as Clone R2 in the middle panel, the average signal ratio of Cluster B_T was also lower than that of Cluster A_T without exception.[72] As shown in the scattergram of the signal ratios in non-cancerous renal tissue samples and RCCs for all examined patients for a representative BAC clone, Clone R3, the DNA methylation status of the non-cancerous renal tissue was basically inherited by the corresponding RCC in individual patients (right panel).[72]

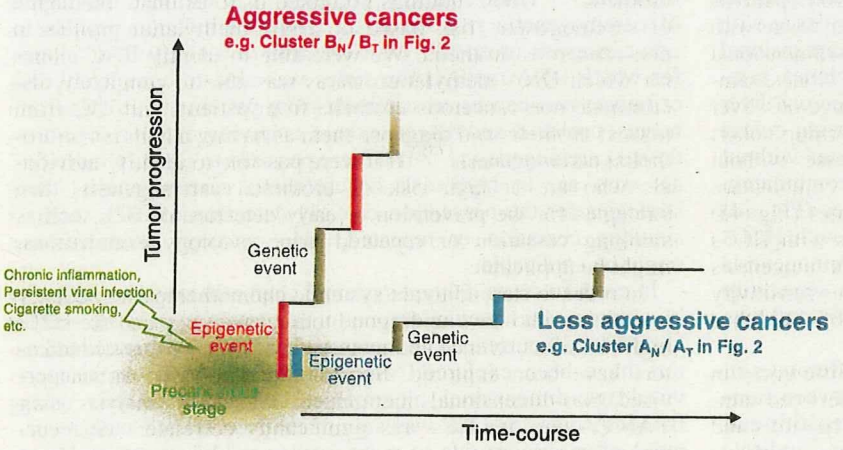

Fig. 3. Significance of DNA methylation alterations at the precancerous stage. Chronic inflammation, persistent infection with viruses or other pathogenic microorganisms, cigarette smoking, exposure to chemical carcinogens, and other unknown factors may participate in the establishment of particular DNA methylation profiles, such as Cluster B_N in Fig. 2. Such DNA methylation alterations in precancerous conditions may not occur randomly, but may be prone to further accumulation of epigenetic and genetic alterations (regional DNA hypermethylation of C-type CpG islands and copy number alterations were accumulated in Cluster B_T in Fig. 2),[72] thus generating more malignant cancers, such as the renal cell carcinomas in patients belonging to Cluster B_T.

doi: 10.1111/j.1349-7006.2009.01383.x

CpG islands was significantly higher in Cluster B_T based on BAMCA than in Cluster A_T. The frequency of CIMP in Cluster B_T was significantly higher than that in Cluster A_T. Genome-wide DNA methylation alterations consisting of both hypo- and hypermethylation revealed by BAMCA in Cluster B_T were associated with regional DNA hypermethylation of C-type CpG islands. For comparison with their DNA methylation status, we also examined copy number alterations by array-based comparative genomic hybridization. By unsupervised hierarchical clustering analysis based on copy number alterations, RCCs were clustered into the two subclasses, clusters A_{TG} and B_{TG}. Loss of chromosome 3p and gain of chromosomes 5q and 7 were frequent in both clusters A_{TG} and B_{TG}. Loss of chromosomes 1p, 4, 9, 13q, and 14q was frequent only in Cluster B_{TG}, and not in Cluster A_{TG}.[74] RCCs showing higher histological grades, renal vein tumor thrombi, vascular involvement and higher pathological TNM stages were accumulated in Cluster B_{TG}. The recurrence-free and overall survival rates of patients in Cluster B_{TG} were significantly lower than those of patients in Cluster A_{TG}.[74] A subclass of Cluster B_T based on BAMCA data was completely included in Cluster B_{TG} showing accumulation of copy number alterations. Genetic and epigenetic alterations are not mutually exclusive during renal carcinogenesis, and particular DNA methylation profiles may be closely related to chromosomal instability. DNA methylation alterations at the precancerous stage, which may not occur randomly but may foster further epigenetic and genetic alterations, can generate more malignant cancers and even determine patient outcome (Fig. 3).

Carcinogenetic risk estimation and prognostication based on DNA methylation status. In samples of non-cancerous liver tissue obtained from patients with HCCs, many BAC clones show DNA hypo- or hypermethylation in comparison with normal liver tissue from patients without HCCs (Fig. 4a).[75] The effectiveness of surgical resection for HCC is limited, unless the disease is diagnosed early at the asymptomatic stage. Therefore, surveillance at the precancerous stage is a priority for patients with HBV or HCV infection. To reveal the baseline liver histology, microscopic examination of liver biopsy specimens is carried out in patients with HBV or HCV infection prior to interferon therapy.[76,77] Carcinogenetic risk estimation using such liver biopsy specimens is advantageous for close follow-up of patients who are at high risk of HCC development. To establish an indicator for carcinogenetic risk estimation, we first omitted potentially insignificant BAC clones associated only with inflammation and/or fibrosis and focused on BAC clones for which DNA methylation status was altered at the precancerous stage in comparison to normal liver tissue and was inherited by HCCs themselves from the precancerous stage (Fig. 4b). Among the BAC clones studied, a bioinformatics approach further identified the top 25 for which DNA methylation status was able to discriminate non-cancerous liver tissue from patients with HCCs in the learning cohort from normal liver tissue with sufficient sensitivity and specificity.[75] By two-dimensional hierarchical clustering analysis using these 25 BAC clones, samples of normal liver tissue and samples of non-cancerous liver tissue obtained from patients with HCCs in the learning cohort were successfully subclassified into different subclasses without any error (Fig. 4c). The criteria established using a combination of the DNA methylation status of the 25 BAC clones (Fig. 4d) diagnosed non-cancerous liver tissue from patients with HCCs in the learning cohort as being at high risk of carcinogenesis with a sensitivity and specificity of 100%.[75] The sensitivity and specificity in the validation cohort were both 96%, and thus our criteria were successfully validated.[75]

It was confirmed that there were no significant differences in the number of BAC clones satisfying our criteria between samples of non-cancerous liver tissue showing chronic hepatitis and samples of non-cancerous liver tissue showing cirrhosis, indicating that our criteria were not associated with the degree of inflammation or fibrosis.[75] In addition, the average numbers of BAC clones satisfying our criteria were significantly lower in liver tissue samples from patients with HBV or HCV infection but without HCCs than in samples of non-cancerous liver tissue obtained from patients with HCCs.[75] Therefore, our criteria may be applicable for classifying liver tissue samples obtained from patients who are being followed up because of HBV or HCV infection, chronic hepatitis, or cirrhosis into those that may generate HCCs and those that will not. We intend to validate the reliability of such risk estimation prospectively using liver biopsy specimens obtained prior to interferon therapy from a large cohort of patients with HBV or HCV infection.

To establish criteria for prognostication of patients with HCCs, in the learning cohort, patients who had survived more than 4 years after hepatectomy and patients who had suffered recurrence within 6 months and died within a year after hepatectomy were defined as a favorable-outcome group and a poor-outcome group, respectively. Wilcoxon test revealed that the signal ratios of 41 BAC clones differed significantly between the two groups.[75] Two-dimensional hierarchical clustering analysis using the 41 BAC clones successfully subclassified HCCs in the favorable-outcome group and the poor-outcome group into different subclasses without any error (Fig. 5a). We also established cut-off values for the 41 BAC clones that allowed discrimination of samples between the poor-outcome and favorable-outcome groups with sufficient sensitivity and specificity (Fig. 5b). Multivariate analysis revealed that satisfying our criteria for 32 or more BAC clones was a predictor of overall patient outcome and was independent of parameters that are already known to have prognostic significance,[75] such as histological differentiation, and presence of portal vein tumor thrombi, intrahepatic metastasis, and multicentricity.[33] The cancer-free and overall survival rates of patients with HCCs satisfying the criteria for 32 or more BAC clones in the validation cohort were significantly lower than those of patients with HCCs satisfying the criteria for less than 32 BAC clones (Fig. 5c).[75] Such prognostication using liver biopsy specimens obtained before transarterial embolization, transarterial chemoembolization, and radiofrequency ablation may be advantageous even for patients who undergo such therapies.

As mentioned above, even non-cancerous urothelia showing no remarkable histological changes obtained from patients with UCs may be exposed to carcinogens in urine. In fact, genome-wide DNA methylation profiles of non-cancerous urothelia obtained from patients with nodular invasive UCs showing an aggressive clinical course were inherited by the nodular invasive UCs themselves, suggesting that DNA methylation alterations that were correlated with the development of more malignant invasive cancers had already accumulated in non-cancerous urothelia.[78] These findings prompted us to estimate the degree of carcinogenetic risk based on DNA methylation profiles in non-cancerous urothelia. We were able to identify BAC clones for which DNA methylation status was able to completely discriminate non-cancerous urothelia from patients with UCs from normal urothelia and diagnose them as having a high risk of urothelial carcinogenesis.[78] If it were possible to identify individuals who are at high risk of urothelial carcinogenesis, then strategies for the prevention or early detection of UCs, such as smoking cessation or repeated urine cytology examinations, might be applicable.

In order to start adjuvant systemic chemotherapy immediately in patients who have undergone total cystectomy and are still at high risk of recurrence and metastasis of UCs, prognostic indicators have been explored. Subclassification based on unsupervised two-dimensional hierarchical clustering analysis using BAMCA data for UCs was significantly correlated with recurrence after surgery due to metastasis to pelvic lymph nodes or

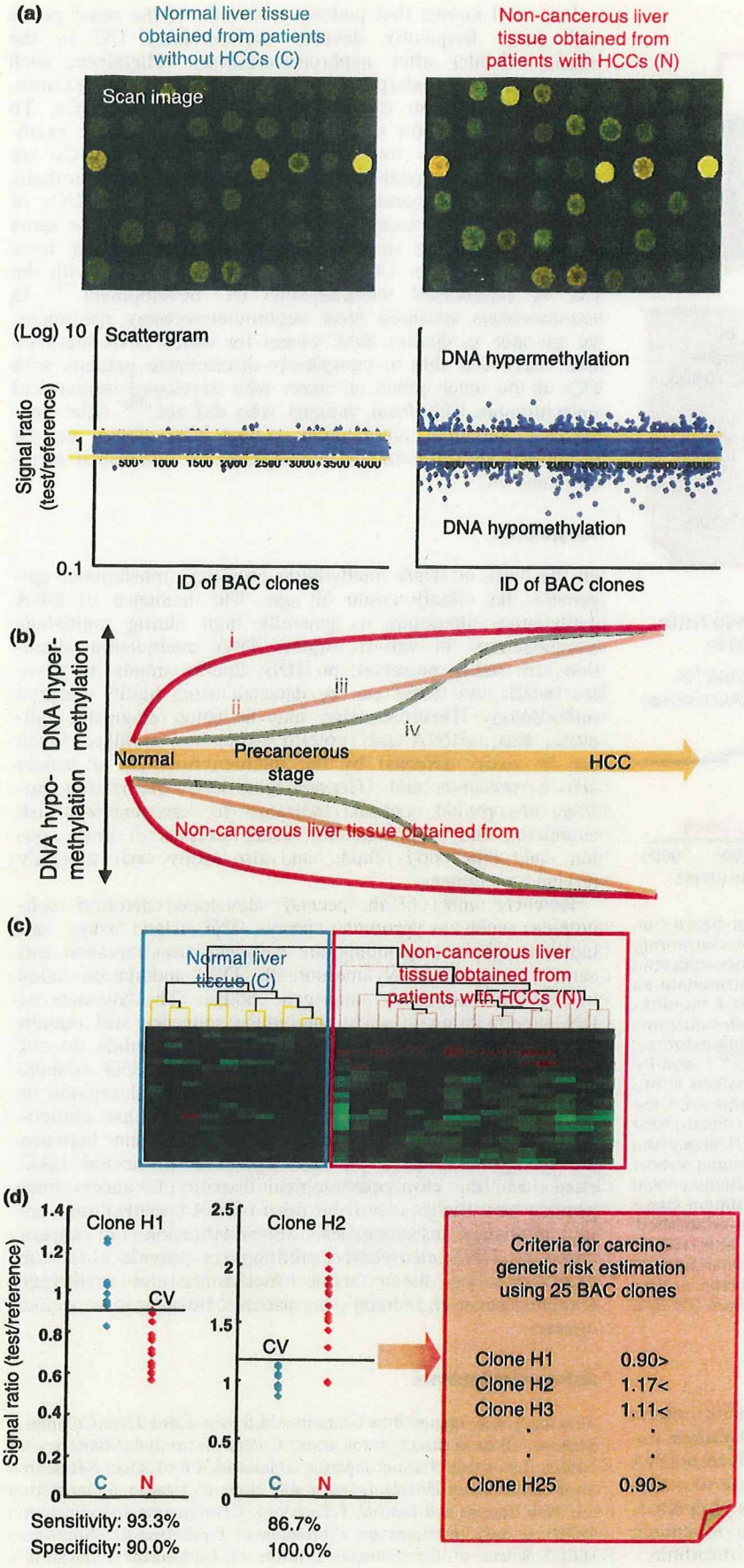

Fig. 4. Risk estimation of hepatocellular carcinoma (HCC) development based on DNA methylation status. (a) Examples of scan images and scattergrams of signal ratios in normal liver tissue obtained from patients without HCCs (C) and non-cancerous liver tissue obtained from patients with HCCs (N). In N samples, many bacterial artificial chromosome (BAC) clones showed DNA hypo- or hypermethylation compared to C samples.[75] (b) Four patterns of DNA methylation alterations seen in BAC clones during multistage hepatocarcinogenesis: (i) DNA methylation alterations occurred at the chronic hepatitis and liver cirrhosis stage, and DNA methylation status did not alter in HCCs from the chronic hepatitis and liver cirrhosis stage; (ii) DNA methylation alterations occurred at the chronic hepatitis and liver cirrhosis stage and further altered in HCCs; (iii) although DNA methylation alterations occurred at the chronic hepatitis and liver cirrhosis stage, the DNA methylation status returned to normal in HCCs; and (iv) DNA methylation alterations occurred only in HCCs. In order to establish criteria for carcinogenetic risk estimation, we focused on BAC clones whose DNA methylation status was inherited by HCCs from the precancerous stage (groups i and ii), whereas group iii may only reflect inflammation and/or fibrosis, and group iv may participate only in the malignant progression stage. (c) Two-dimensional hierarchical clustering analysis using BAC clones that were selected as the top 25 for which DNA methylation status was able to discriminate N from C with sufficient sensitivity and specificity by Wicoxon test and the support vector machine algorithm.[75] C and N samples in the learning cohort were successfully subclassified into different subclasses without any error.[75] (d) Scattergrams of the signal ratios in C and N samples in the learning cohort for representative BAC clones, Clone H1 and Clone H2. Using the cut-off values (CV) in each panel, N samples in the learning cohort were discriminated from C samples with sufficient sensitivity and specificity.[75] Based on a combination of DNA methylation status for the 25 BAC clones, the criteria for carcinogenetic risk estimation were established. Using these criteria, the sensitivity and specificity for diagnosis of N samples in the learning cohort as being at high risk of carcinogenesis were both 100%.[75] The sensitivity and specificity in the validation cohort were both 96%, and thus the criteria were successfully validated.[75]

doi: 10.1111/j.1349-7006.2009.01383.x

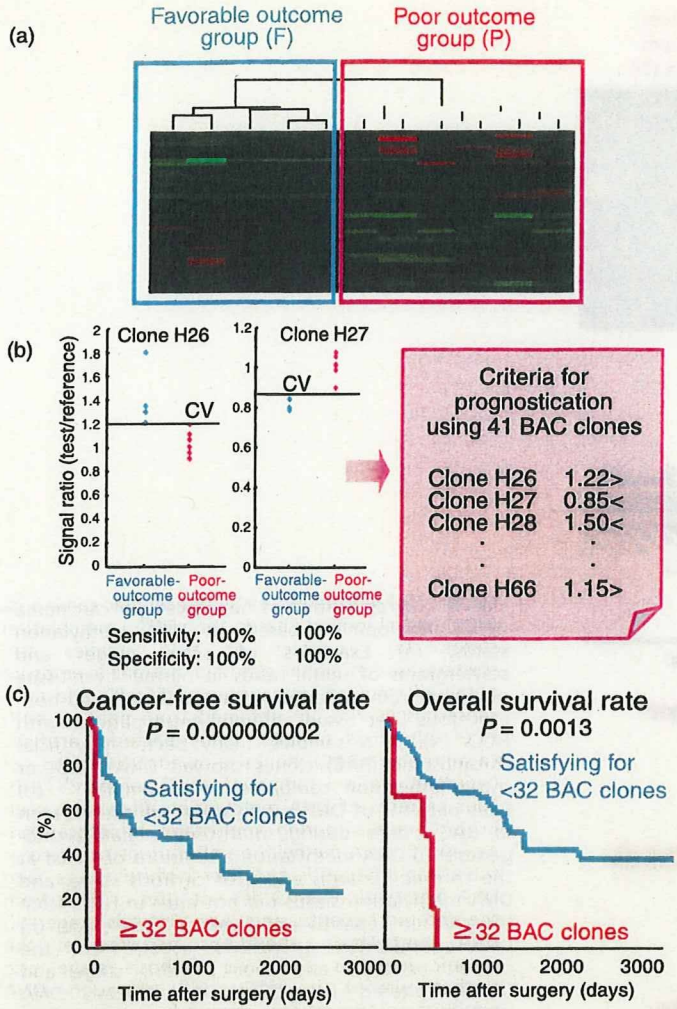

Fig. 5. Prognostication of patients with HCC development based on DNA methylation status. (a) Two-dimensional hierarchical clustering analysis using 41 bacterial artificial chromosome (BAC) clones selected as those for which DNA methylation status was able to discriminate a poor-outcome group (P), who suffered recurrence within 6 months and died within a year after hepatectomy, from a favorable-outcome group (F), who survived for more than 4 years after hepatectomy, with sufficient sensitivity and specificity by Wilcoxon test.[75] F and P patients in the learning cohort were successfully subclassified into different subclasses without any error.[75] (b) Scattergrams of the signal ratios in F and P patients in the learning cohort for representative BAC clones, Clone H26 and Clone H27. Using the cut-off values (CV) in each panel, P patients in the learning cohort were discriminated from F patients with 100% sensitivity and specificity.[75] Based on a combination of the DNA methylation status of the 41 BAC clones, criteria for prognostication were established. (c) The cancer-free and overall survival rates of patients with HCCs in the validation cohort. Patients with HCCs satisfying the criteria for 32 or more BAC clones showed significantly poorer outcome than patients with HCCs satisfying the criteria for less than 32 BAC clones.[75]

distant organs.[78] These data prompted us to establish criteria for predicting recurrence of UCs based on DNA methylation status, and we successfully identified BAC clones for which DNA methylation status completely discriminated patients who suffered recurrence from patients who did not, whereas high histological grade, invasive growth, and vascular or lymphatic involvement were unable to achieve such complete discrimination.[78]

It is well known that patients with UCs of the renal pelvis and ureter frequently develop metachronous UC in the urinary bladder after nephroureterectomy. Therefore, such patients need to undergo repeated urethrocystoscopic examinations for detection of intravesical metachronous UCs. To decrease the need for such invasive urethrocystoscopic examinations, indicators for intravesical metachronous UCs are needed. DNA methylation profiles of non-cancerous urothelia obtained by nephroureterectomy from patients with UCs of the renal pelvis or ureter, which may be exposed to the same carcinogens in the urine as non-cancerous urothelia from which metachronous UCs originate, were correlated with the risk of intravesical metachronous UC development.[78] In non-cancerous urothelia from nephroureterectomy specimens, we are able to identify BAC clones for which DNA methylation status was able to completely discriminate patients with UCs of the renal pelvis or ureter who developed intravesical metachronous UCs from patients who did not.[78] After prospective validation, combination of such BAC clones may be an optimal indicator for the development of intravesical metachronous UC.

Perspective

On the basis of DNA methylation profiling, translational epigenetics has clearly come of age. The incidence of DNA methylation alterations is generally high during multistage carcinogenesis in various organs. DNA methylation alterations are stably preserved on DNA double strands by covalent bonds, and these can be detected using highly sensitive methodology. Therefore, they may be better diagnostic indicators than mRNA and protein expression profiles, which can be easily affected by the microenvironment of cancer cells or precursor cells. Genome-wide DNA methylation profiling can provide optimal indicators for carcinogenetic risk estimation and prognostication using samples of urine, sputum, and other body fluids, and also biopsy and surgically resected specimens.

However, most of the recently developed detection technologies such as promoter arrays, CpG-island arrays and high-throughput sequencing are sequence-based methods and cannot comprehensively measure the DNA methylation status of repetitive sequences and gene bodies. The dynamics of DNA methylation at such non-unique sequences still remain to be determined.[79] Our BAC array-based methods do not focus only on specific promoter regions and CpG islands, and have successfully identified the chromosomal regions in which coordinated DNA methylation alterations have clinicopathological impact. Evaluation of the correlation between the methylation status of each CpG site in selected BAC clones and the clinicopathological diversity of cancers may provide new insights into the roles of DNA methylation during multistage carcinogenesis. Subclassification of cancers based on DNA methylation profiling may provide clues for clarification of distinct target mechanisms and molecules for prevention and therapy in patients belonging to specific clusters.

Acknowledgments

This study was supported by a Grant-in-Aid for the Third Term Comprehensive 10-Year Strategy for Cancer Control from the Ministry of Health, Labor and Welfare of Japan, a Grant-in-Aid for Cancer Research from the Ministry of Health, Labor and Welfare of Japan, a Grant from the New Energy and Industrial Technology Development Organization (NEDO), and the Program for Promotion of Fundamental Studies in Health Sciences of the National Institute of Biomedical Innovation (NiBio).

Abbreviations

BAC	bacterial artificial chromosome
BAMCA	BAC array-based methylated CpG island amplification
CIMP	CpG island methylator phenotype
DNMT	DNA methyltransferase
HBV	hepatitis B virus
HCC	hepatocellular carcinoma
HCV	hepatitis C virus
LOH	loss of heterozygosity
PanIN	pancreatic intraductal neoplasia
PCNA	proliferating cell nuclear antigen
RCC	renal cell carcinoma
UC	urothelial carcinoma

References

1 Delcuve GP, Rastegar M, Davie JR. Epigenetic control. *J Cell Physiol* 2009; **219**: 243–50.
2 Hermann A, Gowher H, Jeltsch A. Biochemistry and biology of mammalian DNA methyltransferases. *Cell Mol Life Sci* 2004; **61**: 2571–87.
3 Bestor T, Laudano A, Mattaliano R, Ingram V. Cloning and sequencing of a cDNA encoding DNA methyltransferase of mouse cells. The carboxyl-terminal domain of the mammalian enzymes is related to bacterial restriction methyltransferases. *J Mol Biol* 1988; **203**: 971–83.
4 Chuang LS, Ian HI, Koh TW, Ng HH, Xu G, Li BF. Human DNA-(cytosine-5) methyltransferase-PCNA complex as a target for p21WAF1. *Science* 1997; **277**: 1996–2000.
5 Baylin SB. Tying it all together: epigenetics, genetics, cell cycle, and cancer. *Science* 1997; **277**: 1948–9.
6 Bestor TH. The DNA methyltransferases of mammals. *Hum Mol Genet* 2000; **9**: 2395–402.
7 Okano M, Bell DW, Haber DA, Li E. DNA methyltransferases Dnmt3a and Dnmt3b are essential for de novo methylation and mammalian development. *Cell* 1999; **99**: 247–57.
8 Cedar H, Bergman Y. Linking DNA methylation and histone modification: patterns and paradigms. *Nat Rev Genet* 2009; **10**: 295–304.
9 Jones PL, Veenstra GJ, Wade PA *et al.* Methylated DNA and MeCP2 recruit histone deacetylase to repress transcription. *Nat Genet* 1998; **19**: 187–91.
10 Nan X, Ng HH, Johnson CA *et al.* Transcriptional repression by the methyl-CpG-binding protein MeCP2 involves a histone deacetylase complex. *Nature* 1998; **393**: 386–9.
11 Kanai Y, Ushijima S, Nakanishi Y, Hirohashi S. Reduced mRNA expression of the DNA demethylase, MBD2, in human colorectal and stomach cancers. *Biochem Biophys Res Commun* 1999; **264**: 962–6.
12 Esteve PO, Chin HG, Smallwood A *et al.* Direct interaction between DNMT1 and G9a coordinates DNA and histone methylation during replication. *Genes Dev* 2006; **20**: 3089–103.
13 Fuks F, Hurd PJ, Deplus R, Kouzarides T. The DNA methyltransferases associate with HP1 and the SUV39H1 histone methyltransferase. *Nucleic Acids Res* 2003; **31**: 2305–12.
14 Suzuki MM, Bird A. DNA methylation landscapes: provocative insights from epigenomics. *Nat Rev Genet* 2008; **9**: 465–76.
15 Laird PW, Jackson-Grusby L, Fazeli A *et al.* Suppression of intestinal neoplasia by DNA hypomethylation. *Cell* 1995; **81**: 197–205.
16 Eden A, Gaudet F, Waghmare A, Jaenisch R. Chromosomal instability and tumors promoted by DNA hypomethylation. *Science* 2003; **300**: 455.
17 Yoshiura K, Kanai Y, Ochiai A, Shimoyama Y, Sugimura T, Hirohashi S. Silencing of the E-cadherin invasion-suppressor gene by CpG methylation in human carcinomas. *Proc Natl Acad Sci USA* 1995; **92**: 7416–9.
18 Jones PA, Baylin SB. The fundamental role of epigenetic events in cancer. *Nat Rev Genet* 2002; **3**: 415–28.
19 Baylin SB, Ohm JE. Epigenetic gene silencing in cancer – a mechanism for early oncogenic pathway addiction? *Nat Rev Cancer* 2006; **6**: 107–16.
20 Gronbaek K, Hother C, Jones PA. Epigenetic changes in cancer. *Apmis* 2007; **115**: 1039–59.
21 Jones PA, Baylin SB. The epigenomics of cancer. *Cell* 2007; **128**: 683–92.
22 Esteller M. Epigenetics in cancer. *N Engl J Med* 2008; **358**: 1148–59.
23 Shibata D. Inferring human stem cell behaviour from epigenetic drift. *J Pathol* 2009; **217**: 199–205.
24 Ohm JE, McGarvey KM, Yu X *et al.* A stem cell-like chromatin pattern may predispose tumor suppressor genes to DNA hypermethylation and heritable silencing. *Nat Genet* 2007; **39**: 237–42.
25 Pogribny IP, Beland FA. DNA hypomethylation in the origin and pathogenesis of human diseases. *Cell Mol Life Sci* 2009; **66**: 2249–61.
26 Laird PW. The power and the promise of DNA methylation markers. *Nat Rev Cancer* 2003; **3**: 253–66.
27 Issa JP, Kantarjian HM. Targeting DNA methylation. *Clin Cancer Res* 2009; **15**: 3938–46.
28 Kanai Y, Hirohashi S. Alterations of DNA methylation associated with abnormalities of DNA methyltransferases in human cancers during transition from a precancerous to a malignant state. *Carcinogenesis* 2007; **28**: 2434–42.
29 Kanai Y. Alterations of DNA methylation and clinicopathological diversity of human cancers. *Pathol Int* 2008; **58**: 544–58.
30 Tsuda H, Zhang WD, Shimosato Y *et al.* Allele loss on chromosome 16 associated with progression of human hepatocellular carcinoma. *Proc Natl Acad Sci USA* 1990; **87**: 6791–4.
31 Kanai Y, Ushijima S, Tsuda H, Sakamoto M, Sugimura T, Hirohashi S. Aberrant DNA methylation on chromosome 16 is an early event in hepatocarcinogenesis. *Jpn J Cancer Res* 1996; **87**: 1210–7.
32 Kanai Y, Ushijima S, Tsuda H, Sakamoto M, Hirohashi S. Aberrant DNA methylation precedes loss of heterozygosity on chromosome 16 in chronic hepatitis and liver cirrhosis. *Cancer Lett* 2000; **148**: 73–80.
33 Hirohashi S, Ishak KG, Kojiro M *et al.* Hepatocellular carcinoma. In: Hamilton SR, Altonen LA, eds. *World Health Organization classification of tumours. Pathology and genetics. Tumours of the digestive system.* Lyon: IARC Press, 2000; 159–72.
34 Hirohashi S, Kanai Y. Cell adhesion system and human cancer morphogenesis. *Cancer Sci* 2003; **94**: 575–81.
35 Kanai Y, Ushijima S, Hui AM *et al.* The E-cadherin gene is silenced by CpG methylation in human hepatocellular carcinomas. *Int J Cancer* 1997; **71**: 355–9.
36 Kondo Y, Kanai Y, Sakamoto M, Mizokami M, Ueda R, Hirohashi S. Genetic instability and aberrant DNA methylation in chronic hepatitis and cirrhosis – a comprehensive study of loss of heterozygosity and microsatellite instability at 39 loci and DNA hypermethylation on 8 CpG islands in microdissected specimens from patients with hepatocellular carcinoma. *Hepatology* 2000; **32**: 970–9.
37 Peng DF, Kanai Y, Sawada M *et al.* DNA methylation of multiple tumor-related genes in association with overexpression of DNA methyltransferase 1 (DNMT1) during multistage carcinogenesis of the pancreas. *Carcinogenesis* 2006; **27**: 1160–8.
38 Kakizoe T. Development and progression of urothelial carcinoma. *Cancer Sci* 2006; **97**: 821–8.
39 Nakagawa T, Kanai Y, Ushijima S, Kitamura T, Kakizoe T, Hirohashi S. DNA hypermethylation on multiple CpG islands associated with increased DNA methyltransferase DNMT1 protein expression during multistage urothelial carcinogenesis. *J Urol* 2005; **173**: 1767–71.
40 Eguchi K, Kanai Y, Kobayashi K, Hirohashi S. DNA hypermethylation at the D17S5 locus in non-small cell lung cancers: its association with smoking history. *Cancer Res* 1997; **57**: 4913–5.
41 Kanai Y, Ushijima S, Ochiai A, Eguchi K, Hui A, Hirohashi S. DNA hypermethylation at the D17S5 locus is associated with gastric carcinogenesis. *Cancer Lett* 1998; **122**: 135–41.
42 Hodge DR, Peng B, Cherry JC *et al.* Interleukin 6 supports the maintenance of p53 tumor suppressor gene promoter methylation. *Cancer Res* 2005; **65**: 4673–82.
43 Kanai Y, Hui AM, Sun L *et al.* DNA hypermethylation at the D17S5 locus and reduced HIC-1 mRNA expression are associated with hepatocarcinogenesis. *Hepatology* 1999; **29**: 703–9.
44 Sawada M, Kanai Y, Arai E, Ushijima S, Ojima H, Hirohashi S. Increased expression of DNA methyltransferase 1 (DNMT1) protein in uterine cervix squamous cell carcinoma and its precursor lesion. *Cancer Lett* 2007; **251**: 211–9.
45 Burgers WA, Blanchon L, Pradhan S, de Launoit Y, Kouzarides T, Fuks F. Viral oncoproteins target the DNA methyltransferases. *Oncogene* 2007; **26**: 1650–5.
46 Kanai Y, Ushijima S, Nakanishi Y, Sakamoto M, Hirohashi S. Mutation of the DNA methyltransferase (DNMT) 1 gene in human colorectal cancers. *Cancer Lett* 2003; **192**: 75–82.
47 Sun L, Hui AM, Kanai Y, Sakamoto M, Hirohashi S. Increased DNA methyltransferase expression is associated with an early stage of human hepatocarcinogenesis. *Jpn J Cancer Res* 1997; **88**: 1165–70.
48 Saito Y, Kanai Y, Sakamoto M, Saito H, Ishii H, Hirohashi S. Expression of mRNA for DNA methyltransferases and methyl-CpG-binding proteins and DNA methylation status on CpG islands and pericentromeric satellite regions during human hepatocarcinogenesis. *Hepatology* 2001; **33**: 561–8.
49 Saito Y, Kanai Y, Nakagawa T *et al.* Increased protein expression of DNA methyltransferase (DNMT) 1 is significantly correlated with the malignant potential and poor prognosis of human hepatocellular carcinomas. *Int J Cancer* 2003; **105**: 527–32.

doi: 10.1111/j.1349-7006.2009.01383.x

50 Peng DF, Kanai Y, Sawada M *et al.* Increased DNA methyltransferase 1 (DNMT1) protein expression in precancerous conditions and ductal carcinomas of the pancreas. *Cancer Sci* 2005; **96**: 403–8.
51 Toyota M, Ahuja N, Ohe-Toyota M, Herman JG, Baylin SB, Issa JP. CpG island methylator phenotype in colorectal cancer. *Proc Natl Acad Sci USA* 1999; **96**: 8681–6.
52 Issa JP. CpG island methylator phenotype in cancer. *Nat Rev Cancer* 2004; **4**: 988–93.
53 Etoh T, Kanai Y, Ushijima S *et al.* Increased DNA methyltransferase 1 (DNMT1) protein expression correlates significantly with poorer tumor differentiation and frequent DNA hypermethylation of multiple CpG islands in gastric cancers. *Am J Pathol* 2004; **164**: 689–99.
54 Kanai Y, Ushijima S, Kondo Y, Nakanishi Y, Hirohashi S. DNA methyltransferase expression and DNA methylation of CPG islands and peri-centromeric satellite regions in human colorectal and stomach cancers. *Int J Cancer* 2001; **91**: 205–12.
55 Ushijima T. Epigenetic field for cancerization. *J Biochem Mol Biol* 2007; **40**: 142–50.
56 Nakagawa T, Kanai Y, Saito Y, Kitamura T, Kakizoe T, Hirohashi S. Increased DNA methyltransferase 1 protein expression in human transitional cell carcinoma of the bladder. *J Urol* 2003; **170**: 2463–6.
57 Wong N, Lam WC, Lai PB, Pang E, Lau WY, Johnson PJ. Hypomethylation of chromosome 1 heterochromatin DNA correlates with q-arm copy gain in human hepatocellular carcinoma. *Am J Pathol* 2001; **159**: 465–71.
58 Nakagawa T, Kanai Y, Ushijima S, Kitamura T, Kakizoe T, Hirohashi S. DNA hypomethylation on pericentromeric satellite regions significantly correlates with loss of heterozygosity on chromosome 9 in urothelial carcinomas. *J Urol* 2005; **173**: 243–6.
59 Hansen RS, Wijmenga C, Luo P *et al.* The DNMT3B DNA methyltransferase gene is mutated in the ICF immunodeficiency syndrome. *Proc Natl Acad Sci USA* 1999; **96**: 14412–7.
60 Saito Y, Kanai Y, Sakamoto M, Saito H, Ishii H, Hirohashi S. Overexpression of a splice variant of DNA methyltransferase 3b, DNMT3b4, associated with DNA hypomethylation on pericentromeric satellite regions during human hepatocarcinogenesis. *Proc Natl Acad Sci USA* 2002; **99**: 10060–5.
61 Soejima K, Fang W, Rollins B. DNA methyltransferase 3b contributes to oncogenic transformation induced by SV40T antigen and activated Ras. *Oncogene* 2003; **22**: 4723–33.
62 Kanai Y, Saito Y, Ushijima S, Hirohashi S. Alterations in gene expression associated with the overexpression of a splice variant of DNA methyltransferase 3b, DNMT3b4, during human hepatocarcinogenesis. *J Cancer Res Clin Oncol* 2004; **130**: 636–44.
63 Estecio MR, Yan PS, Ibrahim AE *et al.* High-throughput methylation profiling by MCA coupled to CpG island microarray. *Genome Res* 2007; **17**: 1529–36.
64 Beck S, Rakyan VK. The methylome: approaches for global DNA methylation profiling. *Trends Genet* 2008; **24**: 231–7.
65 Meissner A, Mikkelsen TS, Gu H *et al.* Genome-scale DNA methylation maps of pluripotent and differentiated cells. *Nature* 2008; **454**: 766–70.
66 Inazawa J, Inoue J, Imoto I. Comparative genomic hybridization (CGH)-arrays pave the way for identification of novel cancer-related genes. *Cancer Sci* 2004; **95**: 559–63.
67 Misawa A, Inoue J, Sugino Y *et al.* Methylation-associated silencing of the nuclear receptor 1I2 gene in advanced-type neuroblastomas, identified by bacterial artificial chromosome array-based methylated CpG island amplification. *Cancer Res* 2005; **65**: 10233–42.
68 Tanaka K, Imoto I, Inoue J *et al.* Frequent methylation-associated silencing of a candidate tumor-suppressor, CRABP1, in esophageal squamous-cell carcinoma. *Oncogene* 2007; **26**: 6456–68.
69 Sugino Y, Misawa A, Inoue J *et al.* Epigenetic silencing of prostaglandin E receptor 2 (PTGER2) is associated with progression of neuroblastomas. *Oncogene* 2007; **26**: 7401–13.
70 Maekita T, Nakazawa K, Mihara M *et al.* High levels of aberrant DNA methylation in Helicobacter pylori-infected gastric mucosae and its possible association with gastric cancer risk. *Clin Cancer Res* 2006; **12**: 989–95.
71 Clark SJ. Action at a distance: epigenetic silencing of large chromosomal regions in carcinogenesis. *Hum Mol Genet* 2007; **16** (Spec No 1): R88–95.
72 Arai E, Ushijima S, Fujimoto H *et al.* Genome-wide DNA methylation profiles in both precancerous conditions and clear cell renal cell carcinomas are correlated with malignant potential and patient outcome. *Carcinogenesis* 2009; **30**: 214–21.
73 Arai E, Kanai Y, Ushijima S, Fujimoto H, Mukai K, Hirohashi S. Regional DNA hypermethylation and DNA methyltransferase (DNMT) 1 protein overexpression in both renal tumors and corresponding nontumorous renal tissues. *Int J Cancer* 2006; **119**: 288–96.
74 Arai E, Ushijima S, Tsuda H *et al.* Genetic clustering of clear cell renal cell carcinoma based on array-comparative genomic hybridization: its association with DNA methylation alteration and patient outcome. *Clin Cancer Res* 2008; **14**: 5531–9.
75 Arai E, Ushijima S, Gotoh M *et al.* Genome-wide DNA methylation profiles in liver tissue at the precancerous stage and in hepatocellular carcinoma. *Int J Cancer* 2009; **125**: 2854–62.
76 Arase Y, Ikeda K, Suzuki F *et al.* Comparison of interferon and lamivudine treatment in Japanese patients with HBeAg positive chronic hepatitis B. *J Med Virol* 2007; **79**: 1286–92.
77 Yoshida H, Tateishi R, Arakawa Y *et al.* Benefit of interferon therapy in hepatocellular carcinoma prevention for individual patients with chronic hepatitis C. *Gut* 2004; **53**: 425–30.
78 Nishiyama N, Arai E, Chihara Y *et al.* Genome-wide DNA methylation profiles in urothelial carcinomas and urothelia at the precancerous stage. *Cancer Sci* 2009; doi: 10.1111/j.1349-7006.2009.01330.x.
79 Mohn F, Schubeler D. Genetics and epigenetics: stability and plasticity during cellular differentiation. *Trends Genet* 2009; **25**: 129–36.

Genome-wide DNA methylation profiles in urothelial carcinomas and urothelia at the precancerous stage

Naotaka Nishiyama,[1,2] Eri Arai,[1] Yoshitomo Chihara,[1] Hiroyuki Fujimoto,[3] Fumie Hosoda,[4] Tatsuhiro Shibata,[4] Tadashi Kondo,[5] Taiji Tsukamoto,[2] Sana Yokoi,[6] Issei Imoto,[6] Johji Inazawa,[6] Setsuo Hirohashi[1] and Yae Kanai[1,7]

[1]Pathology Division, National Cancer Center Research Institute, Tokyo; [2]Urology Division, Sapporo Medical University, Sapporo; [3]Urology Division, National Cancer Center Hospital, Tokyo; [4]Cancer Genomics Project, National Cancer Center Research Institute, Tokyo; [5]Proteome Bioinformatics Project, National Cancer Center Research Institute, Tokyo; [6]Department of Molecular Cytogenetics, Medical Research Institute and School of Biomedical Science, Tokyo Medical and Dental University, Tokyo, Japan

(Received June 16, 2009/Revised August 13, 2009/Accepted August 19, 2009/Online publication September 22, 2009)

To clarify genome-wide DNA methylation profiles during multistage urothelial carcinogenesis, bacterial artificial chromosome (BAC) array-based methylated CpG island amplification (BAMCA) was performed in 18 normal urothelia obtained from patients without urothelial carcinomas (UCs) (C), 17 noncancerous urothelia obtained from patients with UCs (N), and 40 UCs. DNA hypo- and hypermethylation on multiple BAC clones was observed even in N compared to C. Principal component analysis revealed progressive DNA methylation alterations from C to N, and to UCs. DNA methylation profiles in N obtained from patients with invasive UCs were inherited by the invasive UCs themselves, that is DNA methylation alterations in N were correlated with the development of more malignant UCs. The combination of DNA methylation status on 83 BAC clones selected by Wilcoxon test was able to completely discriminate N from C, and diagnose N as having a high risk of carcinogenesis, with 100% sensitivity and specificity. The combination of DNA methylation status on 20 BAC clones selected by Wilcoxon test was able to completely discriminate patients who suffered from recurrence after surgery from patients who did not. The combination of DNA methylation status for 11 BAC clones selected by Wilcoxon test was able to completely discriminate patients with UCs of the renal pelvis or ureter who suffered from intravesical metachronous UC development from patients who did not. Genome-wide alterations of DNA methylation may participate in urothelial carcinogenesis from the precancerous stage to UC, and DNA methylation profiling may provide optimal indicators for carcinogenetic risk estimation and prognostication. (*Cancer Sci* 2010; 101: 231–240)

It is known that DNA hypomethylation results in chromosomal instability as a result of changes in chromatin structure, and that DNA hypermethylation of CpG islands silences tumor-related genes in cooperation with histone modification in human cancers.[1–5] Accumulating evidence suggests that alterations of DNA methylation are involved even in the early and the precancerous stages.[6,7] On the other hand, in patients with cancers, aberrant DNA methylation is significantly associated with poorer tumor differentiation, tumor aggressiveness, and poorer patient outcome.[6,7] Therefore, alterations of DNA methylation may play a significant role in multistage carcinogenesis.

With respect to urothelial carcinogenesis, we have reported accumulation of DNA methylation on C-type CpG islands in a cancer-specific but not age-dependent manner, and protein overexpression of DNA methyltransferase (DNMT) 1, a major DNMT, even in noncancerous urothelia with no apparent histological changes obtained from patients with urothelial carcinomas (UCs).[8,9] Moreover, accumulation of DNA methylation on C-type CpG islands associated with DNMT1 protein overexpression was more frequently evident in aggressive nodular invasive UCs[8–10] resulting in poorer patient outcome than in superficial papillary UCs, which usually remain noninvasive even after repeated urethrocystoscopic resection.[11,12] Since aberrant DNA methylation is one of the earliest molecular events during urothelial carcinogenesis and also participates in tumor aggressiveness, it may be possible to estimate the future risk of developing more malignant UCs. However, only a few previous studies focusing on UCs[13] have employed recently developed array-based technology for assessing genome-wide DNA methylation status,[14–16] and such studies have focused on identification of tumor-related genes that are silenced by DNA methylation.[13] DNA methylation profiles, which could become the optimum indicators for carcinogenetic risk estimation and prognostication of UCs, should therefore be explored using array-based approaches.

In this study, in order to clarify genome-wide DNA methylation profiles during multistage urothelial carcinogenesis, we performed bacterial artificial chromosome (BAC) array-based methylated CpG island amplification (BAMCA)[17–19] using a microarray of 4361 BAC clones[20] in normal urothelia obtained from patients without UCs, noncancerous urothelia obtained from patients with UCs, and UCs themselves.

Materials and Methods

Patients and tissue samples. Seventeen samples of noncancerous urothelia (N1–N17) and 40 samples of UCs (T1–T40) of the urinary bladder, ureter, and renal pelvis were obtained from specimens that had been surgically resected by radical cystectomy (12 patients) or nephroureterectomy (28 patients) at the National Cancer Center Hospital, Tokyo, Japan. The patients comprised 31 men and nine women whose mean age was 69.03 ± 9.77 (mean ± SD) years (range, 49–85 years). Microscopic examination revealed no remarkable histological changes in the noncancerous urothelia. The patients from whom noncancerous urothelia were obtained comprised 11 men and six women with a mean age of 70.41 ± 9.33 (mean ± SD) years (range, 49–85 years). There were 17 superficial UCs (two pTa and 15 pT1 tumors) and 23 invasive UCs (six pT2, 16 pT3, and one pT4 tumor) according to the criteria proposed by World Health Organization classification.[21] For comparison, 18 samples of normal urothelia obtained from patients without UCs (C1–C18) were used. Fourteen, three, and one patient underwent nephrectomy for renal cell carcinoma, nephrectomy for retroperitoneal sarcoma around the kidney, and partial cystectomy for urachal carcinoma, respectively. The patients from whom normal urothelia were obtained comprised 13 men and five women with a mean age of 61.17 ± 15.16 (mean ± SD) years (range, 27–82 years). This study was approved by the Ethics Committee of the National Cancer Center, Tokyo, Japan and has

[7]To whom correspondence should be addressed. E-mail: ykanai@ncc.go.jp

doi: 10.1111/j.1349-7006.2009.01330.x

been performed in accordance with the Declaration of Helsinki in 1995. All patients gave their informed consent prior to their inclusion in this study.

BAMCA. High-molecular-weight DNA from fresh frozen tissue samples was extracted using phenol-chloroform, followed by dialysis. Because DNA methylation status is known to be organ-specific,[22] the reference DNA for analysis of the developmental stages of UCs should be obtained from the urothelium, and not from other organs or peripheral blood. Therefore, a mixture of normal urothelial DNA obtained from 11 male patients (C19–C29) and six female patients (C30–C35) without UCs was used as a reference for analyses of male and female test DNA samples, respectively. DNA methylation status was analyzed by BAMCA using a custom-made array (MCG Whole Genome Array-4500) harboring 4361 BAC clones located throughout chromosomes 1–22, X and Y,[20] as described previously.[17–19] Briefly, 5-μg aliquots of test or reference DNA were first digested with 100 units of the methylation-sensitive restriction enzyme Sma I and subsequently with 20 units of the methylation-insensitive Xma I. Adapters were ligated to the Xma I-digested sticky ends, and PCR was performed with an adapter primer set. Test and reference PCR products were labeled by random priming with Cy3- and Cy5-dCTP (GE Healthcare, Buckinghamshire, UK), respectively, and precipitated together with ethanol in the presence of Cot-I DNA. The mixture was applied to array slides and incubated at 43°C for 72 h. Arrays were scanned with a GenePix Personal 4100A (Axon Instruments, Foster City, CA, USA) and analyzed using GenePix Pro 5.0 imaging software (Axon Instruments) and Acue 2 software (Mitsui Knowledge Industry, Tokyo, Japan). The signal ratios were normalized in each sample to make the mean signal ratios of all BAC clones 1.0.

Statistics. Differences in the average number of BAC clones that showed DNA methylation alterations (DNA hypo- and hypermethylation) between groups of samples were analyzed using the Mann–Whitney *U*-test. Differences at $P < 0.05$ were considered significant. Principal component analysis based on BAMCA data was performed using the Expressionist software program (Gene Data, Basel, Switzerland). Unsupervised two-dimensional hierarchical clustering analysis of tissue samples and the BAC clones were performed using the Expressionist software program. Correlations between the subclassification of patients yielded by unsupervised hierarchical clustering analysis and clinicopathological parameters of UCs were analyzed using the χ^2-test. Differences at $P < 0.05$ were considered significant. BAC clones whose signal ratios yielded by BAMCA were significantly different between groups of samples were identified by Wilcoxon test ($P < 0.01$).

Results

Genome-wide DNA methylation alterations during multistage urothelial carcinogenesis. Figure 1(b,c) shows examples of scanned array images and scattergrams of the signal ratios (test signal/reference signal), respectively, for normal urothelium from a patient without UC (panel C), and both noncancerous urothelium (panel N) and cancerous tissue (panel T) from a patient with UC. In all normal urothelia (C1–C18), the signal ratios of 97% of the BAC clones were between 0.67 and 1.5 (red bars in Fig. 1c). Therefore, in noncancerous urothelia obtained from patients with UCs and UCs, DNA methylation status corresponding to a signal ratio of less than 0.67 and more than 1.5 was defined as DNA hypomethylation and DNA hypermethylation of each BAC clone compared to normal urothelia, respectively, as in our previous study.[23] In noncancerous urothelia obtained from patients with UCs, many BAC clones showed DNA hypo- or hypermethylation (panel N of Fig. 1c). In UCs themselves, more BAC clones showed DNA hypo- or hypermethylation, and the degree of DNA hypo- or hypermethylation, that is deviation of the signal ratio from 0.67 or 1.5, was increased (panel T of Fig. 1c) in comparison with noncancerous urothelia obtained from patients with UCs. The average number of BAC clones showing DNA hypomethylation increased significantly from noncancerous urothelia obtained from patients with UCs (24.53 ± 31.48) to UCs (236.78 ± 92.78, $P = 4.37e\text{-}9$). The average number of BAC clones showing DNA hypermethylation increased significantly from noncancerous urothelia obtained from patients with UCs (29.18 ± 39.84) to UCs (289.13 ± 82.42, $P = 7.35e\text{-}9$). Principal component analysis based on BAMCA data (signal ratios) revealed progressive DNA methylation alterations from normal urothelia, to noncancerous urothelia obtained from patients with UCs, and to UCs (Fig. 1d).

Clinicopathological significance of DNA methylation alterations in noncancerous urothelia obtained from patients with UCs. In order to clarify the clinicopathological significance of DNA methylation alterations in noncancerous urothelia obtained from patients with UCs, unsupervised two-dimensional hierarchical clustering analysis based on BAMCA data (signal ratios) for noncancerous urothelia was performed. Seventeen patients with UCs were clustered into two subclasses, Clusters A_N and B_N, which contained nine and eight patients, respectively, based on the DNA methylation status of the noncancerous urothelia (Fig. 2a). All eight patients (100%) belonging to Cluster B_N suffered from invasive UCs (pT2 or more), whereas five (55.6%) of the patients belonging to Cluster A_N did so ($P = 0.0311$).

The Wilcoxon test ($P < 0.01$) revealed that the signal ratios of 131 BAC clones differed significantly between noncancerous urothelia obtained from patients with superficial UCs (pTa and pT1) and noncancerous urothelia obtained from patients with invasive UCs (pT2 or more). If the average signal ratios in noncancerous urothelia obtained from patients with invasive UCs were significantly higher than those in noncancerous urothelia obtained from patients with superficial UCs (67 BAC clones), the average signal ratios in the invasive UCs themselves were even higher than (42 BAC clones, e.g. RP11-79K14 and RP11-29C11 in Fig. 2b) or not significantly different from (25 BAC clones, e.g. RP11-3A9 and RP11-73G16 in Fig. 2b) those in noncancerous urothelia obtained from patients with invasive UCs, without exception. If the average signal ratios in noncancerous urothelia obtained from patients with invasive UCs were significantly lower than those in noncancerous urothelia obtained from patients with superficial UCs (64 BAC clones), the average signal ratios in the invasive UCs themselves were even lower than (38 BAC clones, e.g. RP11-210F15 and RP11-368O13 in Fig. 2b) or not significantly different from (26 BAC clones, e.g. RP11-442N24 and RP11-65C22 in Fig. 2b) those in noncancerous urothelia obtained from patients with invasive UCs, without exception, that is DNA methylation status of the 131 BAC clones in noncancerous urothelia obtained from patients with invasive UCs was inherited by the invasive UCs themselves.

DNA methylation profiles discriminating noncancerous urothelia obtained from patients with UCs from normal urothelia. Our finding that DNA methylation alterations in noncancerous urothelia were correlated with the development of UCs, as described above, prompted us to estimate the degree of carcinogenetic risk based on DNA methylation profiles in noncancerous urothelia. We attempted to establish criteria for indicating that noncancerous urothelia obtained from patients with UCs, and not normal urothelia, were at high risk of carcinogenesis.

The Wilcoxon test ($P < 0.01$) revealed that the signal ratios on 201 BAC clones differed significantly between normal urothelia obtained from patients without UCs and noncancerous urothelia obtained from patients with UCs. Figure 3(a) shows

doi: 10.1111/j.1349-7006.2009.01330.x

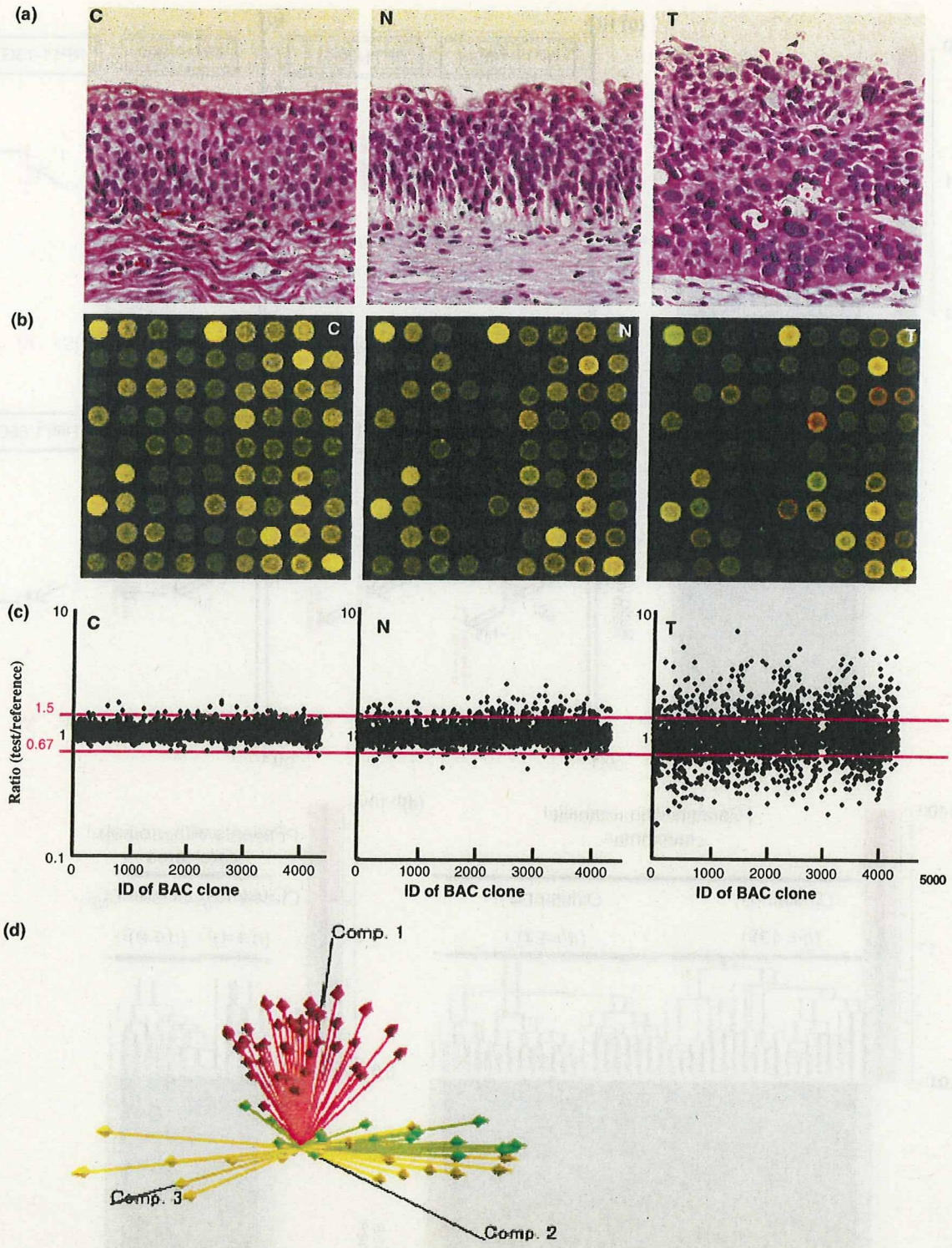

Fig. 1. DNA methylation alterations during multistage urothelial carcinogenesis. (a) Microscopic view of normal urothelium obtained from a patient without urothelial carcinoma (UC) (C), noncancerous urothelium obtained from a patient with UC (N), and UC (T). N shows no remarkable histological changes in comparison to C, that is no cytological or structural atypia is evident. Hematoxylin–eosin staining. Original magnification, ×20. (b) Scanned array images obtained by bacterial artificial chromosome (BAC) array-based methylated CpG island amplification (BAMCA) in C, N, and T. Co-hybridization was done with test and reference DNA labeled with Cy3 and Cy5, respectively. (c) Scattergrams of the signal ratios (test signal/reference signal) obtained by BAMCA in C, N, and T. In all 18 normal urothelia (C1–C18), the signal ratios of 97% of the BAC clones were between 0.67 and 1.5 (red bars). Therefore, in N and T, DNA methylation status corresponding to a signal ratio of less than 0.67 and more than 1.5 was defined as DNA hypomethylation and DNA hypermethylation on each BAC clone compared to C, respectively. Even though N did not show any marked histological changes in comparison to C (panels C and N in [a]), many BAC clones showed DNA hypo- or hypermethylation. In T, more BAC clones showed DNA hypo- or hypermethylation, whose degree, that is deviation of the signal ratio from 0.67 or 1.5, was increased in comparison to N. (d) Principal component analysis based on BAMCA data (signal ratios). Progressive alterations of DNA methylation status from normal urothelia (yellow arrows) to noncancerous urothelia obtained from patients with UCs (green arrows), and to UCs (red arrows) were observed.

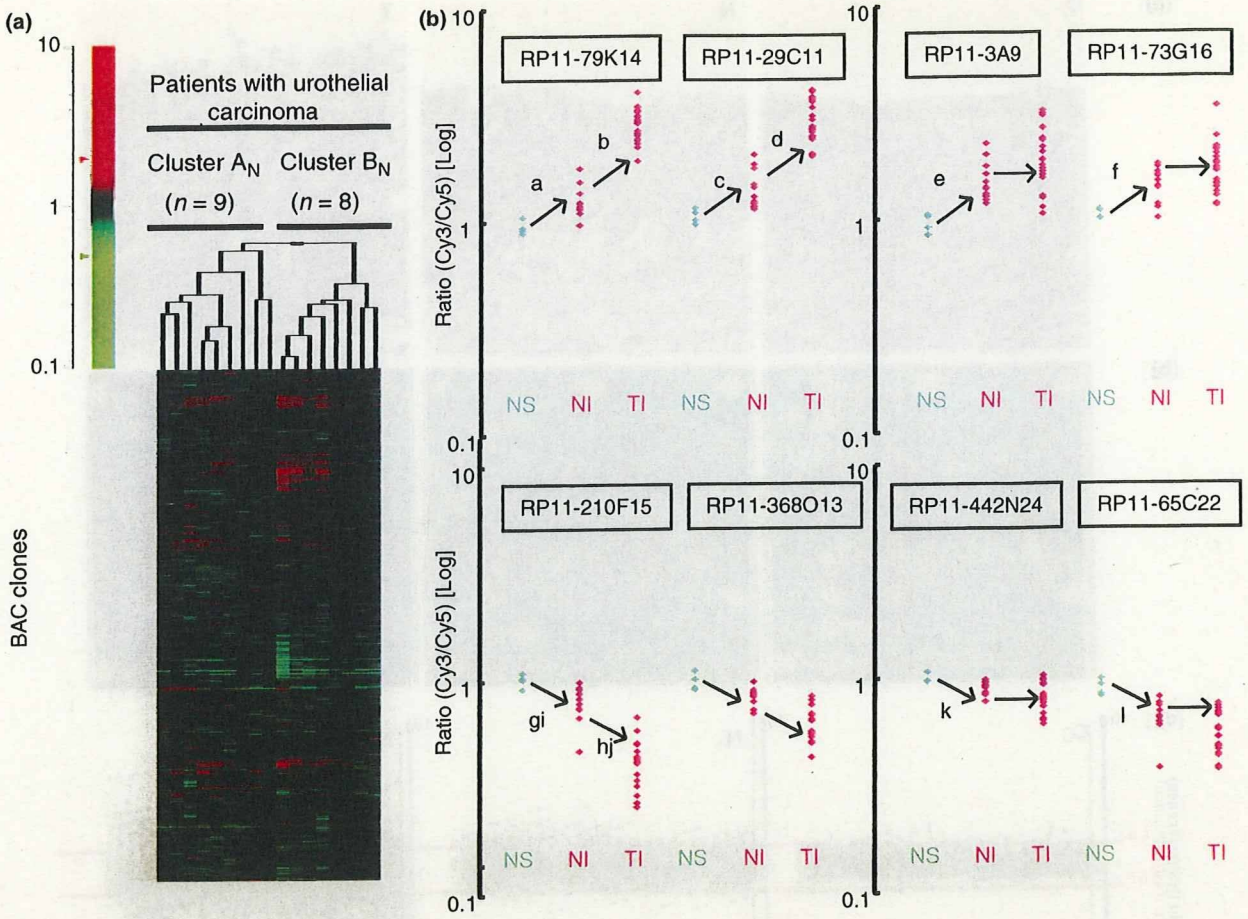

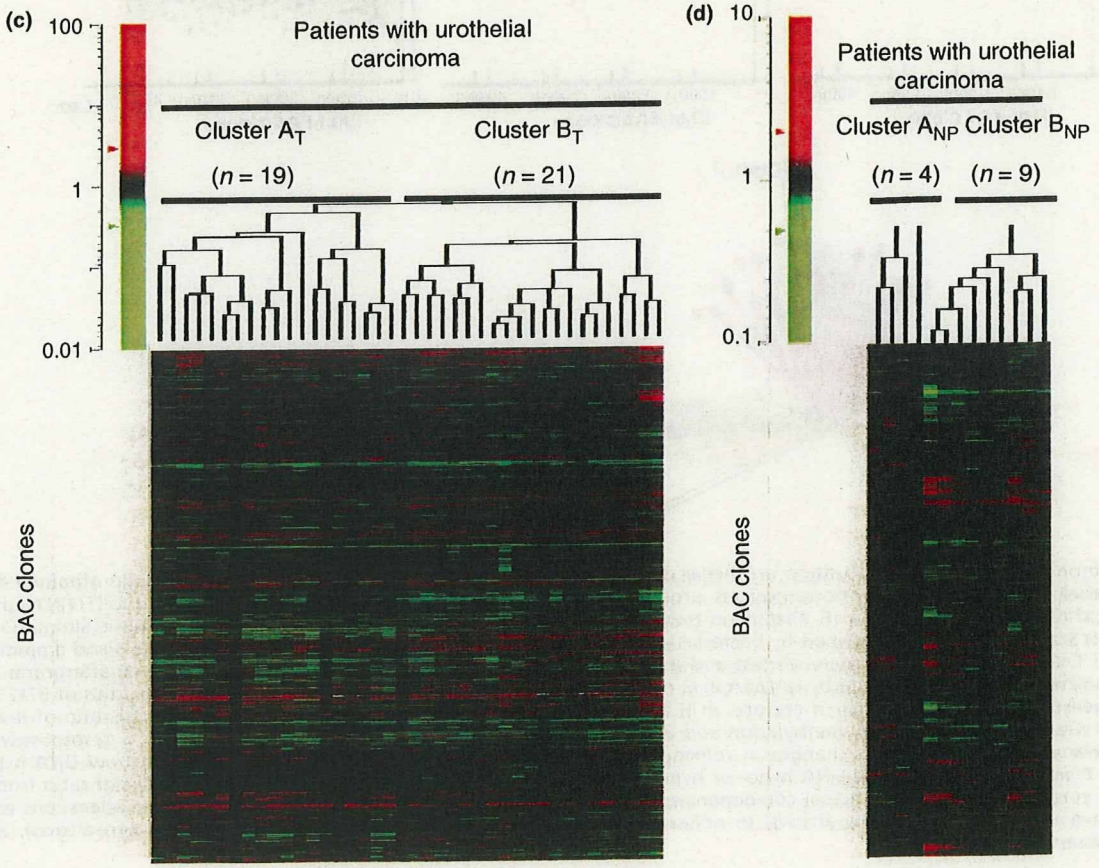

doi: 10.1111/j.1349-7006.2009.01330.x

Fig. 2. Correlations between DNA methylation status and clinicopathological parameters. (a) Unsupervised two-dimensional hierarchical clustering analysis based on bacterial artificial chromosome (BAC) array-based methylated CpG island amplification (BAMCA) data (signal ratios) in noncancerous urothelia obtained from patients with urothelial carcinomas (UCs). The signal ratio is shown in the color range map. Seventeen patients with UCs were hierarchically clustered into two subclasses, Clusters A_N (n = 9) and B_N (n = 8). Eight patients (100%) belonging to Cluster B_N developed invasive UCs (pT2 or more), whereas five patients (55.6%) belonging to Cluster A_N did so (P = 0.0311). (b) Scattergrams of the signal ratios in tissue samples. NS, noncancerous urothelia obtained from patients with superficial UCs. NI, noncancerous urothelia obtained from patients with invasive UCs. TI, invasive UCs. If the average signal ratios in NI were significantly higher than those in NS, the average signal ratios in TI themselves were even higher than (BAC clones RP11-79K14 and RP11-29C11), or not significantly different from (BAC clones RP11-3A9 and RP11-73G16), those in NI without exception. If the average signal ratios in NI were significantly lower than those in NS, the average signal ratios in TI themselves were even lower than (BAC clones RP11-210F15 and RP11-368O13), or not significantly different from (BAC clones RP11-442N24 and RP11-65C22), those in NI without exception. ^{a}P = 0.001680673, ^{b}P = 9.23504e-7, ^{c}P = 0.002197802, ^{d}P = 3.64223e-6, ^{e}P = 0.000840336, ^{f}P = 0.007692306, ^{g}P = 0.004395604, ^{h}P = 8.31509e-6, ^{i}P = 0.004395604, ^{j}P = 1.10173e-5, ^{k}P = 0.005882353, ^{l}P = 0.001098901. (c) Unsupervised two-dimensional hierarchical clustering analysis based on BAMCA data (signal ratios) in UCs. Forty patients with UCs were hierarchically clustered into two subclasses, Clusters A_T (n = 19) and B_T (n = 21). All four patients with recurrence belonged to Cluster B_T. (d) Unsupervised two-dimensional hierarchical clustering analysis based on BAMCA data (signal ratios) for noncancerous urothelia obtained from patients with UCs of the renal pelvis or ureter. Thirteen patients with UCs of the renal pelvis or ureter were hierarchically clustered into two subclasses, Clusters A_{NP} (n = 4) and B_{NP} (n = 9). All four patients who developed intravesical metachronous UC belonged to Cluster B_{NP}.

scattergrams of the signal ratios in normal urothelia and noncancerous urothelia obtained from patients with UCs for representative examples of the 201 BAC clones. Using the cut-off values described in Figure 3(a), noncancerous urothelia obtained from patients with UCs were discriminated from normal urothelia with sufficient sensitivity and specificity (Fig. 3a). From the 201 BAC clones, 83 for which such discrimination was performed with a sensitivity and specificity of 75% or more than 75% were selected (Table S1). The cut-off values of the signal ratios for the 83 BAC clones, and their sensitivity and specificity, are shown in Table S1.

A histogram showing the number of BAC clones satisfying the criteria listed in Table S1 for 18 normal urothelia (C1–C18) and 17 noncancerous urothelia obtained from patients

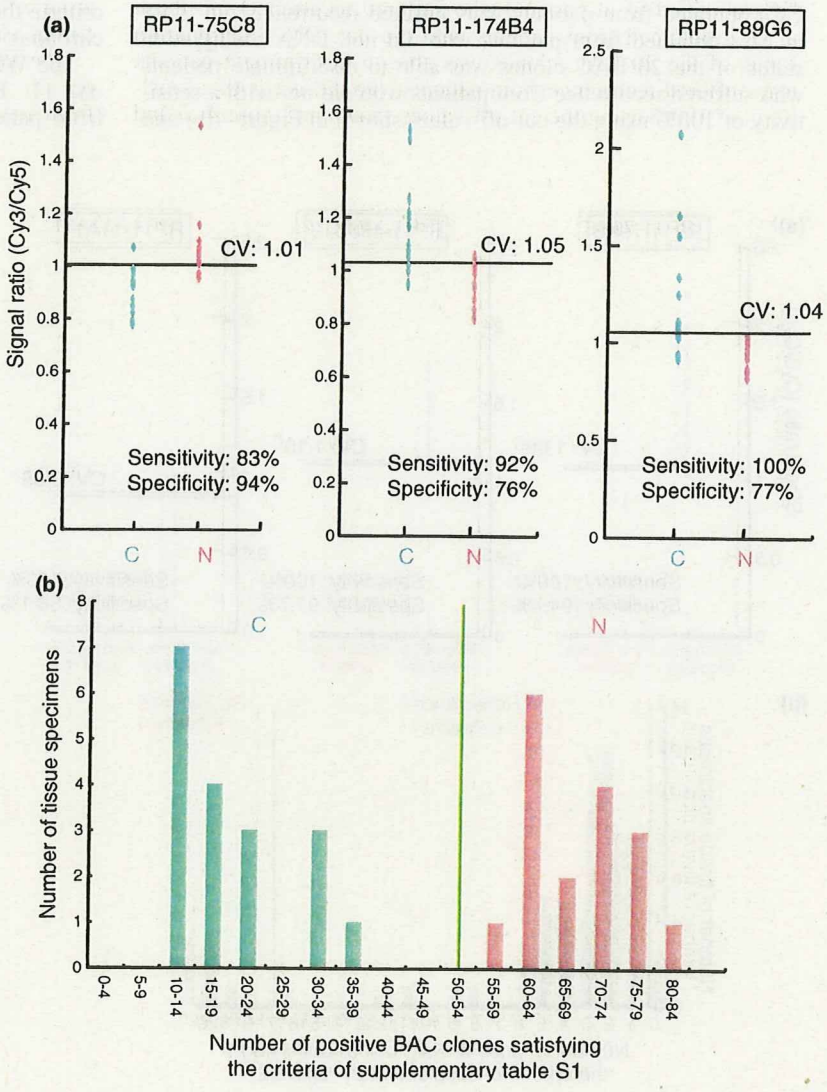

Fig. 3. DNA methylation profiles discriminating noncancerous urothelia obtained from patients with urothelial carcinomas (UCs) (N) from normal urothelia (C). (a) Scattergrams of the signal ratios in C and N on representative bacterial artificial chromosome (BAC) clones, RP11-75C8, RP11-174B4, and RP11-89G6. Using the cut-off values (CV) described in each panel, N in this cohort were discriminated from C with sufficient sensitivity and specificity. (b) Histogram showing the number of BAC clones satisfying the criteria listed in Table S1 in samples C1–C18 and N1–N17. Based on this histogram, we established a criterion that when the noncancerous urothelia satisfied the criteria in Table S1 for 50 (green bar) or more than 50 BAC clones, they were judged to be at high risk of carcinogenesis.

with UCs (N1–N17) is shown in Figure 3(b). Based on this figure, we finally established the following criteria: when noncancerous urothelia satisfied the criteria in Table S1 for 50 or more BAC clones (green bar in Fig. 3b), they were judged to be at high risk of carcinogenesis, and when noncancerous urothelia satisfied the criteria in Table S1 for less than 50 BAC clones, they were judged not to be at high risk of carcinogenesis. Based on these criteria, both the sensitivity and specificity for diagnosis of noncancerous urothelia obtained from patients with UCs in this cohort as being at high risk of carcinogenesis were 100%.

Association of DNA methylation profiles in UCs with recurrence. Unsupervised two-dimensional hierarchical clustering analysis based on BAMCA data (signal ratios) for UCs was able to group 40 patients into two subclasses, Clusters A_T and B_T, which contained 19 and 21 patients, respectively (Fig. 2c). Four patients (19.0%) belonging to Cluster B_T suffered recurrence after surgery (metastasis to the pelvic lymph nodes in three, and metastasis to the lung and bone in one), whereas none (0%) belonging to Cluster A_T did so ($P = 0.0449$). The mean observation period was 29.8 ± 28.0 months (mean ± SD). These data prompted us to establish criteria for predicting recurrence of UCs based on DNA methylation status.

The Wilcoxon test ($P < 0.01$) revealed that the signal ratios on 20 BAC clones in UCs differed significantly between the patients who suffered recurrence after surgery and patients who did not. Figure 4(a) shows scattergrams of the signal ratios in UCs obtained from patients who suffered recurrence and those in UCs obtained from patients who did not. DNA methylation status of the 20 BAC clones was able to discriminate patients who suffered recurrence from patients who did not with a sensitivity of 100% using the cut-off values shown in Figure 4(a) and Table S2. A histogram showing the number of BAC clones satisfying the criteria listed in Table S2 for all 40 UCs is shown in Figure 4(b). Satisfying the criteria in Table S2 for 17 or more BAC clones (green bar in Fig. 4b) discriminated patients who suffered recurrence from patients who did not with a sensitivity and specificity of 100%, whereas high histological grade,[21] invasive growth (pT2 or more), and vascular or lymphatic involvement were unable to achieve such complete discrimination (data not shown).

Association of DNA methylation profiles in noncancerous urothelia obtained from patients with UCs of the renal pelvis or ureter with intravesical metachronous UC development. It is well known that patients with UCs of the renal pelvis and ureter frequently suffer from metachronous UC development in the urinary bladder after nephroureterectomy.[24,25] Since such metachronous UC originates from the noncancerous urothelium of the urinary bladder, we focused on the DNA methylation status of noncancerous urothelia obtained by nephroureterectomy from patients with UCs of the renal pelvis or ureter. Unsupervised two-dimensional hierarchical clustering analysis based on BAMCA data (signal ratios) for noncancerous urothelia obtained from patients with UCs of the renal pelvis or ureter was able to group 13 patients into two subclasses, Clusters A_{NP} and B_{NP}, which contained four and nine patients, respectively (Fig. 2d). Four (44%) of the patients in Cluster B_{NP} developed intravesical metachronous UCs, whereas none (0%) belonging to Cluster A_{NP} did so. These data prompted us to establish criteria that could predict the development of intravesical metachronous UC based on DNA methylation status.

The Wilcoxon test ($P < 0.01$) revealed that the signal ratios on 11 BAC clones in noncancerous urothelia obtained from patients with UCs of the renal pelvis or ureter differed

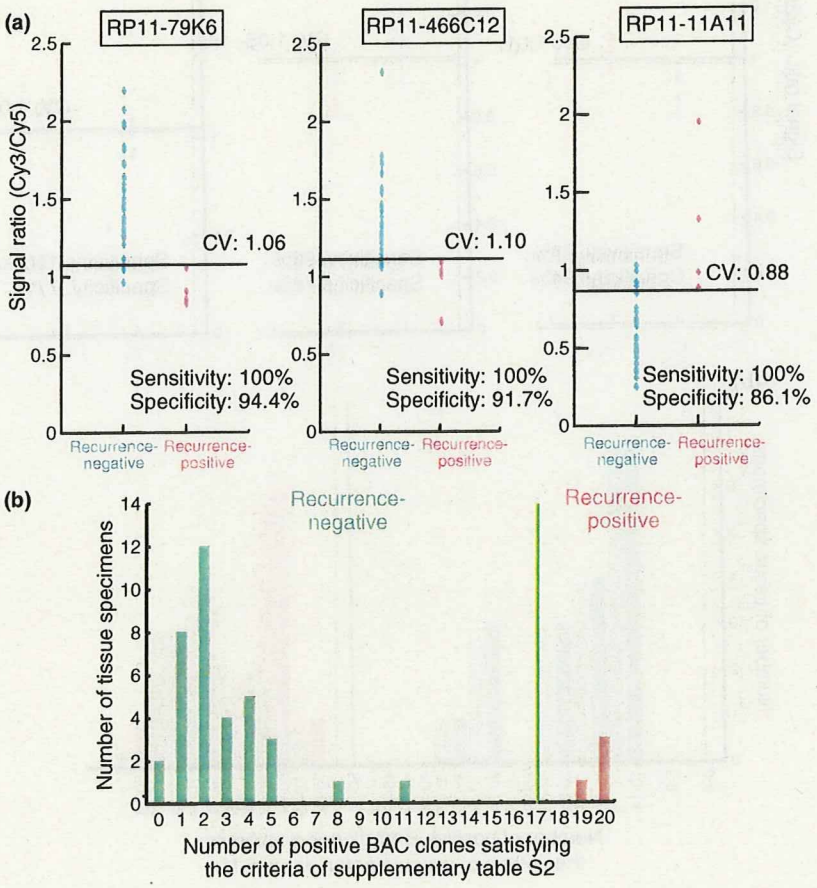

Fig. 4. DNA methylation profiles in urothelial carcinomas (UCs) associated with recurrence. (a) Scattergrams of the signal ratios in UCs from patients who did not develop recurrence ($n = 36$) and UCs from patients who developed recurrence ($n = 4$) on representative bacterial artificial chromosome (BAC), clones, RP11-79K6, RP11-466C12, and RP11-11A11. Using the cut-off values (CV) described in each panel, recurrence-positive patients were discriminated from recurrence-negative patients with 100% sensitivity. (b) Histogram showing the number of BAC clones satisfying the criteria listed in Table S2 in all 40 patients with UCs. Satisfying the criteria in Table S2 for 17 (green bar) or more than 17 BAC clones discriminated recurrence-positive patients from recurrence-negative patients with a sensitivity and specificity of 100%, whereas high histological grade (21), invasive growth (pT2 or more), and vascular or lymphatic involvement were unable to achieve such complete discrimination (data not shown).

doi: 10.1111/j.1349-7006.2009.01330.x

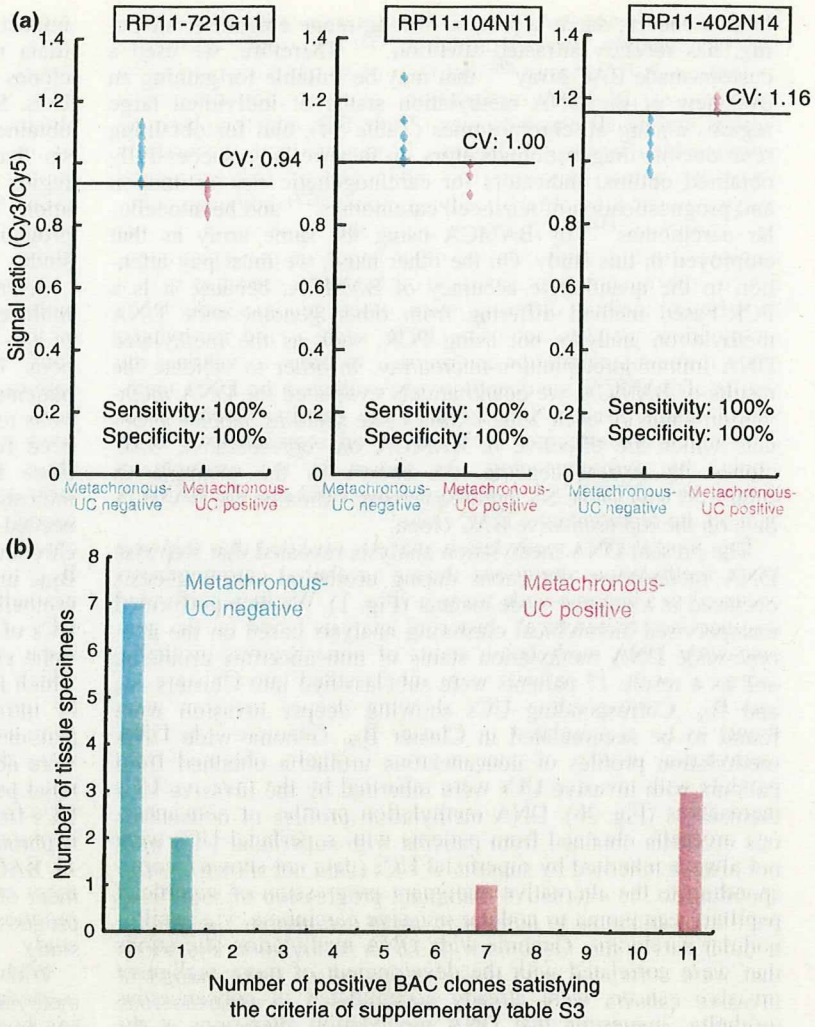

Fig. 5. DNA methylation profiles in noncancerous urothelia obtained from patients with urothelial carcinomas (UCs) of the renal pelvis or ureter associated with intravesical metachronous UC development. (a) Scattergrams of the signal ratios in noncancerous urothelia obtained from patients who did not develop intravesical metachronous UCs ($n = 9$) and noncancerous urothelia obtained from patients who developed intravesical metachronous UCs ($n = 4$) on representative bacterial artificial chromosome (BAC) clones, RP11-721G11, RP11-104N11, and RP11-402N14. Using the cut-off values (CV) described in each panel, metachronous UC-positive patients were discriminated from metachronous UC-negative patients with 100% sensitivity and specificity. (b) Histogram showing the number of BAC clones satisfying the criteria listed in Table S3 in all 13 patients with UCs of the renal pelvis or ureter from whom noncancerous urothelia were obtained. Patients who were negative and positive for metachronous UC were confirmed to show a marked difference in the DNA methylation status of the 11 BAC clones.

significantly between patients who developed intravesical metachronous UC after nephroureterectomy and patients who did not. DNA methylation status of nine of the 11 BAC clones was able to discriminate patients who suffered from intravesical metachronous UC development from patients who did not with a sensitivity and specificity of 100% using the cut-off values shown in Figure 5(a) and Table S3. A histogram showing the number of BAC clones satisfying the criteria listed in Table S3 for 13 noncancerous urothelia obtained from patients with UCs of the renal pelvis or ureter is shown in Figure 5(b).

Discussion

Urothelial carcinomas are clinically remarkable because of their multicentricity: synchronously or metachronously multifocal UCs often develop in individual patients. A possible mechanism for such multiplicity is the "field effect," whereby carcinogenic agents in the urine cause malignant transformation of multiple urothelial cells.[26] Even noncancerous urothelia showing no remarkable histological features obtained from patients with UCs can be considered to be at the precancerous stage, because they may be exposed to carcinogens in the urine. On the other hand, UCs are classified as superficial papillary carcinomas or nodular invasive carcinomas according to their configuration. Superficial papillary carcinomas usually remain noninvasive, although patients need to undergo repeated urethrocystoscopic resections because of recurrences. In contrast, the clinical outcome of nodular invasive carcinomas is poor.[11,12]

In our previous study, accumulation of DNA methylation on C-type CpG islands associated with DNMT1 protein overexpression was observed even in noncancerous urothelia obtained from patients with UCs.[8,9] Aberrant DNA methylation was further increased, especially in nodular invasive carcinomas.[8–10] These previous data suggested that carcinogenetic risk estimation and prognostication of UCs based on DNA methylation status might be a promising strategy. Although optimal diagnostic indicators have never been explored using array-based genome-wide DNA methylation analysis, alterations of DNA methylation on several CpG islands in UCs have been reported separately.[27–31]

Many researchers in the field of cancer epigenetics have used promoter arrays to identify the genes that are methylated in cancer cells.[14–16] However, the promoter regions of specific genes are not the only target of DNA methylation alterations in human cancers. DNA methylation status in genomic regions that do not directly participate in gene silencing, such as the edges of CpG islands, may be altered at the precancerous stage before the alterations of the promoter regions themselves occur.[32] Genomic regions in which DNA hypomethylation affects chromosomal instability may not be contained in promoter arrays. Moreover, aberrant DNA methylation of large regions of chromosomes, which are regulated in a coordinated manner in